

Smoothing splines for discontinuous signals

Martin Storath*, Andreas Weinmann†

September 20, 2023

Abstract

Smoothing splines are twice differentiable by construction, so they cannot capture potential discontinuities in the underlying signal. In this work, we consider a special case of the weak rod model of Blake and Zisserman (1987) that allows for discontinuities penalizing their number by a linear term. The corresponding estimates are cubic smoothing splines with discontinuities (CSSD) which serve as representations of piecewise smooth signals and facilitate exploratory data analysis. However, computing the estimates requires solving a non-convex optimization problem. So far, efficient and exact solvers exist only for a discrete approximation based on equidistantly sampled data. In this work, we propose an efficient solver for the continuous minimization problem with non-equidistantly sampled data. Its worst case complexity is quadratic in the number of data points, and if the number of detected discontinuities scales linearly with the signal length, we observe linear growth in runtime. This efficient algorithm allows to use cross validation for automatic selection of the hyperparameters within a reasonable time frame on standard hardware. We provide a reference implementation and supplementary material. We demonstrate the applicability of the approach for the aforementioned tasks using both simulated and real data.

*Lab for Mathematical Methods in Computer Vision and Machine Learning, Technische Hochschule Würzburg-Schweinfurt, Schweinfurt, Germany.

†Department of Mathematics and Natural Sciences, Hochschule Darmstadt, Darmstadt, Germany.

1 Introduction

Assume that we are given the approximate values $y_i = g(x_i) + \epsilon_i$ of a function g at data sites x_1, \dots, x_N , and an estimate δ_i of the standard deviation of the errors ϵ_i which are uncorrelated with zero mean. If we can assume that g is a smooth function, then we may try to estimate g using a (cubic) smoothing spline, a flexible and widely-applicable approach to curve estimation (Hastie et al., 2009; Silverman, 1985). Using the notations of De Boor (2001), a cubic smoothing spline is the solution \hat{f} of the variational problem

$$\min_{f \in C^2} p \sum_{i=1}^N \left(\frac{y_i - f(x_i)}{\delta_i} \right)^2 + (1 - p) \int_{x_1}^{x_N} (f''(t))^2 dt. \quad (1)$$

Here, the minimum is taken over all twice continuously differentiable functions on $[x_1, x_N]$. The minimizer is a compromise between the conflicting goals smoothness, measured by the squared euclidean norm of the derivative, and closeness to data. The “stiffness” parameter $p \in (0, 1)$ controls the relative weight of the two goals. It is well known that the minimizer \hat{f} of (1) is a cubic spline, that is, \hat{f} is a piecewise cubic polynomial function which is twice continuously differentiable (De Boor, 2001). If the underlying function g has discontinuities (or breaks/jumps), or in other words, g is only piecewise smooth, the classical smoothing spline cannot capture these discontinuities.

Signals with discontinuities appear in numerous applications; for example, the cross-hybridization of DNA (Drobyshev et al., 2003; Hupé et al., 2004; Snijders et al., 2001), the reconstruction of brain stimuli (Winkler et al., 2005), single-molecule analysis (Joo et al., 2008; Loeff et al., 2021), cellular ion channel functionalities (Hotz et al., 2013), photo-emission spectroscopy (Frick et al., 2014) and the rotations of the bacterial flagellar motor (Sowa et al., 2005); see also Kleinberg and Tardos (2006) and Frick et al. (2014) for further examples.

We are interested in the case where the locations of the discontinuities are unknown. (If the locations of the discontinuities are known a priori, one simply may compute smoothing splines on the intervals between two points of discontinuities.) In their landmark work, Blake and Zisserman (1987) proposed a variational model for this task based on piecewise regression with smoothing splines and linear penalties on the number of jumps and creases, called the *weak rod model*. Here, we study the special case of the weak rod model without creases, and for discrete, potentially non-equidistant, sampling points. Using the above notation

of smoothing splines, it can be formulated as:

$$\min_{f, J} p \sum_{i=1}^N \left(\frac{y_i - f(x_i)}{\delta_i} \right)^2 + (1 - p) \int_{[x_1, x_N] \setminus J} (f''(t))^2 dt + \gamma |J|. \quad (2)$$

Here the minimum is taken over all possible sets of discontinuities between two data sites $J \subset [x_1, x_N] \setminus \{x_1, \dots, x_N\}$ and all functions f that are twice continuously differentiable away from the discontinuities. The last term is a penalty for the number of discontinuities $|J|$ weighted by a parameter $\gamma > 0$. In (2), we search for a global minimizer which consists of a discontinuity set \hat{J} and a piecewise cubic spline \hat{f} with discontinuities at \hat{J} . The solution \hat{f} of the specific minimization problem (2) is a *cubic smoothing spline with discontinuities* which we abbreviate as *CSSD*. A first example of a CSSD is provided in Figure 1. A CSSD may be used for exploratory data analysis, as predictor, and as function estimator; just like a classical smoothing spline (Silverman, 1985), but with the extension that the underlying function may have discontinuities. Additionally, a detected discontinuity can be seen as a type of changepoint.

The considered instance of the weak rod model (2) is interesting and useful on its own, because it comprises two widely used regression models: For sufficiently large γ , a CSSD coincides with the C^2 continuous cubic smoothing spline. In the limit $p \rightarrow 0$, a CSSD tends to a piecewise linear regression function, which were studied e.g. in Kleinberg and Tardos (2006), Friedrich et al. (2008), Storath et al. (2019). If the second order derivative is replaced by the first order derivative in (2), we obtain the Mumford-Shah model (Mumford and Shah, 1989), and the according limit $p \rightarrow 0$ leads to a piecewise constant regression model, also referred to as Potts model (Winkler and Liebscher, 2002; Winkler, 2003), and studied in a series of further works, including the works of Jackson et al. (2005), Boysen et al. (2009), and Killick et al. (2012), to mention only a few.

The literature describes algorithms for a variant of (2) with a discretized roughness penalty for equidistantly sampled data sites, i.e. $x_{i+1} - x_i = \text{const}$ for all i . For solving this discrete problem, Blake and Zisserman (1987) proposed a graduated non-convexity algorithm, an algorithm based on Hopfield's neural model and a Viterbi-type algorithm but these algorithms are not guaranteed to yield a global minimum in general. Straightforward adaption of the slightly different dynamic programming approaches of Blake (1989) or Winkler and Liebscher (2002), one may obtain a global minimizer in cubic worst case time complexity. Storath et al. (2019) proposed an algorithm which solves the discretized problem for equidistantly sampled data in quadratic complexity.

However, restriction to equidistantly sampled data means a major limitation because (i) many types of data can be acquired only with varying distances of the measurements sites, and (ii) even when the data sites are equidistantly sampled, non-equidistant data points occur naturally when performing K -fold cross validation for parameter selection. The present formulation with continuous roughness penalty (2) naturally deals with non-equidistant data sites x_i , but solving it is more challenging than the discrete equidistant setting. There is – to the authors knowledge – no dedicated paper presenting an exact solver for (2). After the reformulation to a reduced search space (see Section 2.2), one may combine methods of dynamic programming (Blake, 1989; Killick et al., 2012; Winkler and Liebscher, 2002) and smoothing splines (Reinsch, 1967), to obtain an exact solver for (2). However, such a “baseline” solver has worst case cubic time complexity, and hence applying it is costly even for problems of moderate size. This hampers in particular usage of standard parameter selection strategies, such as cross validation, since they require solving (2) for numerous model parameters γ and p . The present paper develops an efficient exact solver for (2). Details on the contribution of this paper follow after a further discussion of prior and related work.

1.1 Prior and related work

Blake and Zisserman (1987) have introduced the weak rod model in the context of image processing along with a two-dimensional generalization which they called the weak plate model. Equation (2) is a special case of the weak rod model in the sense that it does not allow creases (corresponding to the weak rod model with a sufficiently high crease penalty), and that it is formulated with a potentially weighted discrete data term which naturally appears when working with sampled data. Blake and Zisserman (1987) utilized the penalty factors $\mu, \alpha > 0$ which are related to the factors p, γ in (2) by $\mu = \sqrt[4]{(1-p)/p}$ and $\alpha = \gamma/p$. (The present paper adopts the p -parametrization used in a standard reference on splines by De Boor (2001).) Blake and Zisserman (1987) have obtained results on scale and sensitivity in discontinuity detection for the fully continuous version. In particular, they derived a contrast threshold referring to the minimum detectable jump height for an isolated bi-infinite step function in dependance of the model parameters which is given by $h_0 = 2^{\frac{3}{4}} \sqrt{\alpha/\mu}$.

If we replace the second order derivative with the first order derivative in Equation (2), we obtain the weak string model which coincides with the one-dimensional case of the famous Mumford-Shah model for edge preserving smoothing (Mumford and Shah, 1985, 1989). This first order model has been investigated

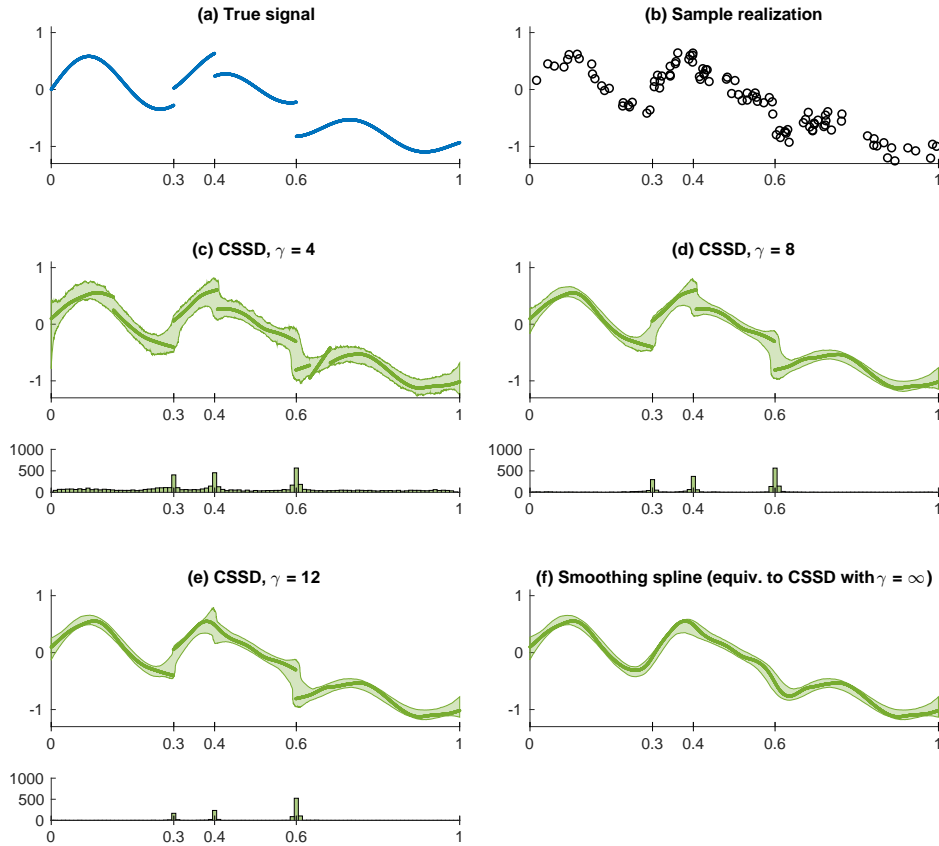


Figure 1: A synthetic signal is sampled at $N = 100$ random data sites x_i and corrupted by zero mean Gaussian noise with standard deviation 0.1. The results of the discussed model are shown for $\rho = 0.999$ and different parameters of γ , where $\gamma = \infty$ corresponds to classical smoothing splines. The thick lines represent the results of the shown sample realization. The x-ticks indicate the true discontinuity locations. The shaded areas depict the 2.5% to 97.5% (pointwise) quantiles of 1000 realizations. The histograms under the plots show the frequency of the detected discontinuity locations over all realizations.

in more detail in the literature than the second order model; in particular, an exact algorithm of cubic complexity for the discretized first order model has been proposed in an early work by Blake (1989). Blake and Zisserman (1987) have described a fundamental limitation of the first order model termed the gradient limit; it refers to the undesired introduction of spurious discontinuities when the gradient exceeds a threshold. The second order model considered here does not have this limitation.

The present model is closely connected to smoothing splines which were de-

veloped in the works of Schoenberg (1964b) and Reinsch (1967), and the basic idea can be tracked back to the work of Whittaker (1923). Silverman (1984) has shown that spline smoothing approximately corresponds to smoothing by a kernel method with bandwidth depending on the local density of the data sites. Comprehensive treatments on smoothing splines are given in the books by De Boor (2001), by Wahba (1990), and by Green and Silverman (1993), as well as in the paper by Silverman (1985). (In the present paper, we use the notations and conventions of De Boor (2001).) The signal and image processing point of view is discussed in the papers of Unser (1999, 2002). Smoothing splines have become a standard method for statistical data processing, and they are discussed in standard literature on the topic (Hastie et al., 2009). Recent contributions on splines in a statistical context are generalizations for Riemannian manifolds (Kim et al., 2021), locally adaptive splines for Bayesian model selection in additive partial linear models (Jeong et al., 2021), knot estimation for linear splines, (Yang et al., 2021), and efficiency improvements for splines with multiple predictors (Meng et al., 2022), to mention only a few.

Besides the above mentioned models of spline-type, many other piecewise regression models with discontinuity or jump penalty have been used. They typically lead to combinatorial optimization problems, and fast solvers are a central question (Frick et al., 2014; Killeck et al., 2012; Winkler and Liebscher, 2002). Efficient algorithms for piecewise constant or piecewise polynomial regression functions have been proposed by Auger and Lawrence (1989), Winkler and Liebscher (2002), Jackson et al. (2005), Friedrich et al. (2008), Little and Jones (2011b), and Killeck et al. (2012), and extended to indirectly measured data (Storath et al., 2014; Weinmann and Storath, 2015) and to non-linear data spaces (Storath et al., 2017; Weinmann et al., 2016). Parallelized versions have been considered by Tickle et al. (2020). For the piecewise constant case, Boysen et al. (2009) have obtained consistency and convergence rates of the estimates in $L^2([0, 1])$. A detailed treatment of piecewise constant regression is given by Little and Jones (2011a,b).

Regarding automatic selection of the model parameters, there are some common approaches for related piecewise regression models; for example information based criteria (Yao, 1988; Zhang and Siegmund, 2007), an interval criterion (Winkler et al., 2005) and several variants of cross validation (Arlot and Celisse, 2011). For classical smoothing splines, generalized cross validation (Craven and Wahba, 1979; Golub et al., 1979; Silverman, 1985) is frequently used. The authors are not aware of an automatic parameter selection strategy specifically developed for the considered model (2).

There are also conceptually different methods for estimating discontinuous

regression functions of spline type. One such approach was proposed by Koo (1997) where knots are stepwise refined by knot addition, basis deletion, knot-merging, and the final model is determined by the Bayes information criterion. Another possibility is a changepoint based approach: one might first use an existing method for changepoint detection to determine discontinuity locations; for example the CUSUM method (Page, 1954), Bayesian changepoint inference (Fearnhead, 2006), wild binary segmentation (Fryzlewicz, 2014), a narrowest over the threshold method (Baranowski et al., 2019), a Bayesian ensemble approach (Zhao et al., 2019), nonparametric maximum likelihood approaches (Haynes et al., 2017; Zou et al., 2014), or multiscale testing (Frick et al., 2014) could be used. (See van den Burg and Williams (2020) and the references therein for an overview and a comparison of selected changepoint detection methods.) Then, splines can be fitted between two detected changepoints; either smoothing splines directly to the data or interpolating splines to the corresponding signal estimates. We point out that such a two stage approach emphasizes the changepoint detection aspect, and as splines are typically not involved in the detection process, they are not necessarily the “natural” models for the data between two changepoints.

For denoising non-smooth signals, shrinkage of wavelet coefficients is frequently used (Donoho and Johnstone, 1994). The book by Mallat (2008) provides an overview on wavelet shrinkage. By their multiscale subdivision algorithms, wavelet methods are computationally extremely efficient. In contrast to the model considered in this work, they typically rely on equidistant sampling points and do not result in piecewise smooth regression functions.

1.2 Contribution

We first discuss basic properties of a CSSD, that is, the properties of the minimizers of (2). In particular, in view of the well-definedness of the estimator, we provide uniqueness results for the optimization problem with respect to both function evaluations and partitions in an almost everywhere sense.

The main contribution of this paper is an efficient algorithm for computing a solution of the problem (2), meaning a global minimum of the target function. The algorithm is developed in three steps: *(i)* We show that we may restrict the search space for the discontinuity set J to the midpoints of the data sites, and we use dynamic programming to reduce the number of possible configurations. *(ii)* We propose a procedure that computes the spline energies for a signal of increasing length in constant time per new element. It allows to obtain the required spline energies on all (discrete) intervals efficiently. We point out that using the

smoothing spline algorithms of Reinsch (1967) and of De Hoog and Hutchinson (1986) lead to significantly higher computational costs for this specific task. *(iii)* We show that the computation of the spline energies is compatible with two different pruning strategies, the PELT pruning of Killick et al. (2012) and the FPVI pruning of Storath and Weinmann (2014). The worst case time complexity of the proposed algorithm is $O(N^2)$ where N is the number of data points. If the number of detected discontinuities scales linearly with N , we observe linear scaling of the runtime.

We provide a ready-to-use reference implementation in Matlab, available for download on Github.¹ The novel solver is notably faster than a baseline solver which relies on standard Python modules and which does not use of the methods developed in the present work. We further implement a strategy for selecting the model parameters (p and γ) automatically based on K -fold cross validation. The proposed fast algorithm allows to perform this selection strategy within a reasonable time frame on standard hardware. Numerical examples with synthetic and real data demonstrate the potential of CSSD as function estimator for discontinuous signals, as basis for a changepoint detector, and as a tool for exploratory data analysis.

2 Efficient computation of a CSSD and uniqueness result

2.1 Reformulation and basic properties of the solutions

Throughout this paper, we assume that the data sites satisfy $x_1 < x_2 < \dots < x_N$. If the data does not satisfy this constraint, we may merge data sites into a single data point by weighted averaging over the y -values of coinciding x -values; see e.g. Hutchinson (1986).

Let $J \subset [x_1, x_N] \setminus \{x_1, \dots, x_N\}$ be a set of discontinuities of size $|J| = K$. It is convenient to sort the elements of J ascendingly so that we can access the elements by an index, e.g. J_1 for the smallest element in J . Its complement in $[x_1, x_N]$ consists of $K + 1$ half open and open intervals, denoted by I_1, \dots, I_{K+1}

$$[x_1, x_N] \setminus J = I_1 \cup \dots \cup I_{K+1}.$$

¹<https://github.com/mstorath/CSSD>

We denote the (ordered) set of these intervals by $\mathcal{P}(J)$

$$\mathcal{P}(J) = \{I_1, \dots, I_{K+1}\}.$$

The minimization problem (2) now can be reformulated equivalently in terms of the discontinuity set and the corresponding intervals as

$$\min_{J \subset [x_1, x_N] \setminus \{x_1, \dots, x_N\}} \sum_{I \in \mathcal{P}(J)} \mathcal{E}_I + \gamma |J| \quad (3)$$

where \mathcal{E}_I is given by

$$\mathcal{E}_I = \min_{f \in C^2(I)} p \sum_{i: x_i \in I} \left(\frac{y_i - f(x_i)}{\delta_i} \right)^2 + (1 - p) \int_I (f''(t))^2 dt. \quad (4)$$

As in (1), the model parameter $p \in (0, 1)$ controls the relative weight of the smoothness term and the data fidelity term, and δ_i is an estimate of the standard deviation of the errors at data site x_i . Note that (4) describes the minimum energy of a classical smoothing spline on the interval I .

A standard procedure to obtain \mathcal{E}_I consists in computing a minimizer f_I of the functional in (4) using the algorithm of Reinsch (1967) on the data in the interval I , and evaluating (4) with that f_I . The computational costs of this approach are linear in the number of data points falling in the interval I . A key element of the fast algorithm we are going to propose in the next section is that it bypasses the costly explicit computation of the f_I , and computes \mathcal{E}_I directly using a recurrence relation.

From (3) we see that every discontinuity set J has a unique piecewise cubic spline function f_J which is defined for all $I \in \mathcal{P}(J)$ by the unique minimizer of (4). So once an optimal discontinuity set is known, the corresponding f_J can be computed by a standard method such as Reinsch's algorithm. In opposite direction, J consists of the discontinuities of f and the discontinuities of f' .

Next we state two basic properties of an optimal discontinuity set \hat{J} .

Lemma 1. *Let \hat{J} be a solution of the minimization problem (3).*

1. \hat{J} has at most one element between two adjacent data sites and
2. \hat{J} has at most $\lceil N/2 \rceil - 1$ elements.

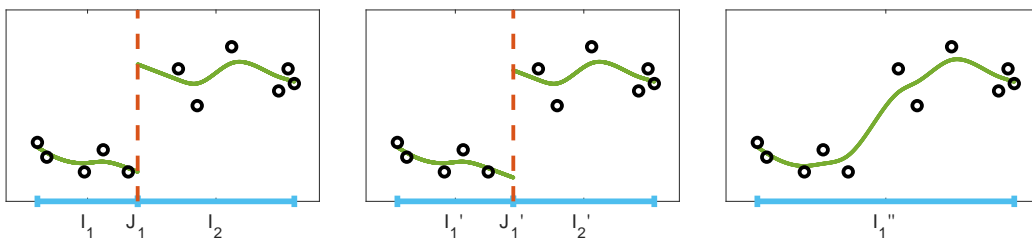


Figure 2: A toy data set (circles) and three possible discontinuity configurations (visualized on abscissa) along with their corresponding piecewise splines (solid curves) are shown (x on abscissa, y on ordinate). The first two configurations give the same function value $\mathcal{E}_{I_1} + \mathcal{E}_{I_2} + \gamma = \mathcal{E}_{I_1'} + \mathcal{E}_{I_2'} + \gamma$, when plugged into the target function in (2). Hence, these configurations are equally good in the sense of the model (2). So we consider the discontinuity locations J_1 and J_1' as equivalent and use the midpoint (here J_1' , middle tile) as natural representative. The third tile shows a configuration with no discontinuity which yields the target function value $\mathcal{E}_{I_1''}$. If γ is sufficiently small ($\gamma < \mathcal{E}_{I_1''} - \mathcal{E}_{I_1} - \mathcal{E}_{I_2}$) the configurations with discontinuity have a better target function value than the one without discontinuity.

The proof is given in the supplementary material.

We develop an efficient solver for (3) – the equivalent formulation of (2) – in three steps: (i) reduction of the search space for the discontinuities to a discrete set and reducing the number of configurations using dynamic programming, (ii) efficient update scheme for the necessary spline energies, (iii) search space pruning which is compatible with the order of computation of the energy updates.

2.2 Reduction of the search space for the discontinuity set

Reducing the discontinuity set to midpoints of data sites. It is a basic property of the classical smoothing spline that its energy \mathcal{E}_I (defined in (4)) only depends on the data sites that are contained in the interval I . The reason for this is that the spline can be extended linearly beyond the extremal data sites without increasing the energy; see e.g. Silverman (1985). So if I and I' are two intervals which contain the same data sites, that is, if $\{x_i : x_i \in I\} = \{x_i : x_i \in I'\}$, then $\mathcal{E}_I = \mathcal{E}_{I'}$. As a direct consequence, a shift of a discontinuity location between two data sites x_i, x_{i+1} does not change the functional value (3). So a discontinuity may be located at an arbitrary position between two data points. Having noticed this, we consider two discontinuity sets as equivalent, if all their respective elements lie between the same data sites. The midpoint between two data sites is a natural choice for a representative of the equivalence class. This is illustrated in Figure 2 using a toy example. Hence, it is sufficient to consider the discrete set of midpoints \mathcal{M} of the

data sites,

$$\mathcal{M} := \{\frac{1}{2}(x_i + x_{i+1}) : i = 1, \dots, N - 1\}, \quad (5)$$

as search space for J . Thus, we have reduced the optimization problem (3) to the discrete optimization problem

$$\min_{J \subset \mathcal{M}} \sum_{I \in \mathcal{P}(J)} \mathcal{E}_I + \gamma|J|. \quad (6)$$

Because \mathcal{M} is a finite set it follows that the minimization problem (6), and so the problems (2) and (3), indeed have a minimizer.

Remark 1. For the algorithm, which we are developing here, the concrete representative of the discontinuity set is irrelevant. The choice of the representative comes into play when displaying the final result. For this purpose, it seems natural to take the midpoints. Yet, there might be scenarios where other points – or even the entire interval – are reasonable representatives for the discontinuity locations. (One may think of a similar situation when dealing with the ordinary median which can be defined as $\operatorname{argmin}_{\mu} |y_i - \mu|$. For data of even length, all values between the two central data points satisfy the minimality property, and most commonly, the mean value between the central points is chosen. However, for implementing the method of Weinmann et al. (2015), considering the upper and lower points as median turned out to be useful.)

Reducing the number of configurations by dynamic programming. The reduced form (6) constitutes a discrete one-dimensional partitioning problem which can be solved by dynamic programming. The approach works similar to the corresponding algorithms on related partitioning problems; see Friedrich et al. (2008); Jackson et al. (2005); Kleinberg and Tardos (2006); Winkler and Liebsher (2002). For completeness we briefly describe the procedure. For the formulation it is convenient, to identify an interval I with the indices of the contained data sites. For example, the interval that contains the data sites x_l, x_{l+1}, \dots, x_r is identified with the (ordered) set of indices $\{l, l + 1, \dots, r\}$, or abbreviated in Matlab-type notation $\{l : r\}$. In particular, we write $\mathcal{E}_{\{l:r\}}$ for \mathcal{E}_I .

We now consider the functional in (6) on a reduced data set $(x_1, y_1), \dots, (x_r, y_r)$ for $r \leq n$ and denote it by F_r ; that is $F_r(J) = \sum_{I \in \mathcal{P}(J)} \mathcal{E}_I + \gamma|J|$, where $J \subset \mathcal{M} \cap [x_1, x_r]$ and \mathcal{E}_I is only evaluated for the data points x_1, \dots, x_r . The minimal functional value of F_r , denoted by $F_r^* = \min_J F_r(J)$, satisfies the Bellman equation

$$F_r^* = \min_{l=1, \dots, r} \left\{ \mathcal{E}_{\{l:r\}} + \gamma + F_{l-1}^* \right\} \quad (7)$$

where we let $F_0^* = -\gamma$, see Friedrich et al. (2008). As $\mathcal{E}_{\{l:r\}} = 0$ for $r - l \leq 1$ and F_l^* non-decreasing in l , the minimum on the right hand side actually only has to be taken over the values $l = 1, \dots, r - 1$. By the dynamic programming principle, we successively compute F_1^*, F_2^* , until we reach F_N^* . As our primary interest are the optimal discontinuities J , rather than the minimal functional values F_N^* , we keep track of these locations. An economic way to do so is to store at step r the minimizing argument l^* of (7) as the value Z_r so that Z encodes the boundaries of an optimal partition. We refer to Friedrich et al. (2008) for a more detailed description of the data structure and a visualization. We record that the number of configurations that have to be checked for computing the minimum value is $O(N^2)$.

2.3 Efficient computation of the spline energies for all intervals

We next develop an efficient procedure to compute the functional values (4) for all discrete intervals $\{l : r\}$ with $1 \leq l \leq r \leq N$. Before starting the development, we discuss why we need a specialized method for this specific task: The algorithm of Reinsch (1967) aims for computing the minimizing argument of (4), and the minimum value has to be computed from that minimizer. This procedure needs linear time for a single value of $\mathcal{E}_{\{l:r\}}$. The method described by De Hoog and Hutchinson (1986) gives direct access to the minimum energy $\mathcal{E}_{\{l:r\}}$ which is achieved by using orthogonal transformations. However, it is designed for fast computation of the energies for different p -parameters for signals of fixed length; no efficient algorithm for signals of increasing lengths is given. Hence, computing a single $\mathcal{E}_{\{l:r\}}$ needs linear time as well. Either approach would result in an algorithm of cubic complexity when used for computing all values $\mathcal{E}_{\{l:r\}}$.

We now develop a specialized method that updates the spline energy on the interval $\{l : r\}$ to that on the interval $\{l : r + 1\}$ in constant time. To keep the notation simple, we describe the procedure for $l = 1$ noting that the procedure works analogously for any other $l = 2, \dots, N$.

Consider the functional in (4) for an interval I which contains exactly the data sites x_1, \dots, x_r , where $2 \leq r \leq N - 1$, and denote its unique minimizing argument by \hat{f}_I . The solution \hat{f}_I is a cubic spline with natural boundary conditions which means that $p_i := \hat{f}_I|_{[x_i, x_{i+1}]}$ is a polynomial of degree at most 3 for all $i = 1, \dots, r - 1$, that \hat{f}_I is in $C^2(I)$, and that $\hat{f}_I''(x_1) = \hat{f}_I''(x_r) = 0$ (De Boor, 2001, Ch. XIV). Let $f, f' \in \mathbb{R}^r$ be the vector of Hermite control points of \hat{f}_I , meaning that $f_i := \hat{f}_I(x_i)$ and, $f'_i := \hat{f}_I'(x_i)$, for $i = 1, \dots, r$. Each polynomial p_i is uniquely determined by f_i, f'_i, f_{i+1} , and f'_{i+1} ; see e.g. (Cheney, 1998, p.61). Hence \hat{f}_I and its $2r$ Hermite

control points f, f' are one-to-one. We may express the polynomials p_i in terms of the Hermite control points as

$$p_i(x) = \sum_{k=0}^3 c_k (x - x_i)^k \quad (8)$$

where $c_0 = f_i, c_1 = f'_i, c_2 = -\frac{f'_{i+1} + 2f'_i}{d_i} + 3\frac{f_{i+1} - f_i}{d_i^2}, c_3 = \frac{f'_{i+1} + f'_i}{d_i^2} + 2\frac{f_i - f_{i+1}}{d_i^3}$, and $d_i = x_{i+1} - x_i$ is the distance between two data sites (Dougherty et al., 1989). Using this representation, we obtain the integral of the square of p'_i on the interval $[x_i, x_{i+1}]$ in terms of f_i, f'_i, f_{i+1} , and f'_{i+1} :

$$\begin{aligned} \int_{x_i}^{x_{i+1}} (p'_i(x))^2 dx = & \frac{12f_i^2}{d_i^3} - \frac{24f_{i+1}f_i}{d_i^3} + \frac{12f_{i+1}^2}{d_i^3} + \frac{12f'_i f_i}{d_i^2} + \frac{12f'_{i+1} f_i}{d_i^2} \\ & - \frac{12f'_i f_{i+1}}{d_i^2} - \frac{12f_{i+1} f'_{i+1}}{d_i^2} + \frac{4(f'_i)^2}{d_i} + \frac{4(f'_{i+1})^2}{d_i} + \frac{4f'_i f'_{i+1}}{d_i}. \end{aligned}$$

This is a quadratic form which can be written in matrix form as $\int_{x_i}^{x_{i+1}} (p'_i(x))^2 dx = v_i^T B v_i$, where $v_i = [f_i, f'_i, f_{i+1}, f'_{i+1}]$ and

$$B_i = \begin{bmatrix} \frac{12}{d_i^3} & \frac{6}{d_i^2} & -\frac{12}{d_i^3} & \frac{6}{d_i^2} \\ \frac{6}{d_i^2} & \frac{4}{d_i} & -\frac{6}{d_i^2} & \frac{2}{d_i} \\ -\frac{12}{d_i^3} & -\frac{6}{d_i^2} & \frac{12}{d_i^3} & -\frac{6}{d_i^2} \\ \frac{6}{d_i^2} & \frac{2}{d_i} & -\frac{6}{d_i^2} & \frac{4}{d_i} \end{bmatrix}.$$

The matrix B_i is symmetric and positive semidefinite with two zero eigenvalues. Invoking a semidefinite variant of the Cholesky decomposition we obtain the factorization

$$B_i = U_i^T U_i, \quad \text{with} \quad U_i = \begin{bmatrix} \frac{2\sqrt{3}}{d_i^{3/2}} & \frac{\sqrt{3}}{\sqrt{d_i}} & -\frac{2\sqrt{3}}{d_i^{3/2}} & \frac{\sqrt{3}}{\sqrt{d_i}} \\ 0 & \frac{1}{\sqrt{d_i}} & 0 & -\frac{1}{\sqrt{d_i}} \end{bmatrix} \in \mathbb{R}^{2 \times 4}. \quad (9)$$

For the next step, it is convenient to decompose U_i as $U_i = [V_i, W_i]$ with $V_i, W_i \in \mathbb{R}^{2 \times 2}$ and to define $e_i^T = [1, 0] \in \mathbb{R}^{1 \times 2}$. Let us define $A^{(r)} \in \mathbb{R}^{2r \times s}$, with $s = 3r - 2$,

by

$$A^{(r)} = \begin{bmatrix} \alpha_1 e_1^T & 0 & 0 & \cdots & 0 \\ \beta V_1 & \beta W_1 & 0 & \cdots & 0 \\ 0 & \alpha_2 e_1^T & 0 & \cdots & 0 \\ 0 & \beta V_2 & \beta W_2 & \cdots & 0 \\ 0 & 0 & \alpha_3 e_1^T & \cdots & 0 \\ \vdots & \ddots & \ddots & \ddots & \vdots \\ 0 & \cdots & 0 & \beta V_{r-1} & \beta W_{r-1} \\ 0 & \cdots & 0 & 0 & \alpha_r e_1^T \end{bmatrix} \quad (10)$$

with $\alpha_i = \frac{\sqrt{p}}{\delta_i}$ and $\beta = \sqrt{1-p}$. Now the optimal functional value $\mathcal{E}_{\{1:r\}}$ can be expressed as follows:

Lemma 2. *Let $\mathcal{E}_{\{1:r\}}$ be given by (4) with $I = \{1 : r\}$. Then,*

$$\mathcal{E}_{\{1:r\}} = \min_{u \in \mathbb{R}^{2r}} \|A^{(r)}u - \tilde{y}^{(r)}\|_2^2, \quad (11)$$

where $A^{(r)}$ is defined in (10), and $\tilde{y}^{(r)} \in \mathbb{R}^s$ is a vector of zeros except $\tilde{y}_{3i-2}^{(r)} = \alpha_i y_i$ for $i = 1, \dots, r$.

The proof is given in the supplementary material.

The form (11) has a key property for our purposes: it is a least squares problem in matrix form so that $A^{(r)}$ is a submatrix of $A^{(r+1)}$ and $\tilde{y}^{(r)}$ is a subvector of $\tilde{y}^{(r+1)}$. This submatrix relation allows us to update the QR-decomposition of the system $[A^{(r)}|\tilde{y}^{(r)}]$ to the QR-decomposition of the system $[A^{(r+1)}|\tilde{y}^{(r+1)}]$ by a constant number of Givens rotations. Let $Q \in \mathbb{R}^{s \times s}$ orthogonal and $R \in \mathbb{R}^{s \times r}$, with $R_{1:r,1:r}$ upper triangular and $R_{r+1:s,1:r} = 0$, such that $A^{(r)} = QR$, and let $z = Q^T \tilde{y}^{(r)}$. Then the minimizer of (11) is the solution of the first r rows of the system

$$[R|z] \quad (12)$$

and $\mathcal{E}_{\{1:r\}}$ is equal to the sum of squares of the last entries, $r+1, \dots, s$, of the right hand side $Q^T \tilde{y}^{(r)}$. Passing from r to $r+1$, extends the system by three rows and two columns:

$$\left[\begin{array}{ccc|c} R_{1:s,1:r-2} & R_{1:s,r-1:r} & 0 & z \\ 0 & \beta V_{r+1} & \beta W_{r+1} & 0 \\ 0 & 0 & \alpha_{r+1} e_1^T & \alpha_{r+1} y_{r+1} \end{array} \right]. \quad (13)$$

This system can be brought to upper triangular form using Givens rotations. By the upper triangular form of R , the Givens rotations only act on the small subsystem

$$\left[\begin{array}{cc|c} R_{r-1:r,r-1:r} & 0 & z_{r-1:r} \\ \beta V_{r+1} & \beta W_{r+1} & 0 \\ 0 & \alpha_{r+1} e_1^T & \alpha_{r+1} y_{r+1} \end{array} \right] \quad (14)$$

where the left hand side is in $\mathbb{R}^{5 \times 4}$. Having applied the Givens rotations, the system has the form $[R'|z']$ with $R' \in \mathbb{R}^{5 \times 4}$, $R'_{1:4,1:4}$ upper triangular and $R'_{5,1:4} = 0$. So the residual is coded in the last entry of z' . Hence we get the update

$$\mathcal{E}_{\{1:r+1\}} = \mathcal{E}_{\{1:r\}} + (z'_5)^2. \quad (15)$$

The update procedure is initialized (for the index $r = 2$) by $\mathcal{E}_{\{1:2\}} = 0$, and the system describing the initial state is given $[R|Q^T \tilde{y}^{(2)}]$ where $QR = A^{(2)}$ is the QR-decomposition of $A^{(2)} \in \mathbb{R}^{4 \times 4}$.

The above derivation leads to the following theorem.

Theorem 3. *The procedure described above (equations (12) to (15)) computes the array $[\mathcal{E}_{\{1:1\}}, \mathcal{E}_{\{1:2\}}, \dots, \mathcal{E}_{\{1:N\}}]$ in $O(N)$ time complexity and $O(N)$ memory complexity.*

The proof is given in the supplementary material.

For any other starting index l with $1 < l \leq r$ the values $\mathcal{E}_{\{l:r\}}$ are computed in the same fashion by calling the above procedure with the starting index l .

A note on the practical implementation seems useful at this point: The described procedure uses Givens rotations for elimination. Unfortunately, by their rowwise action, applying Givens rotations sequentially turns out to be relatively slow when implemented in standard linear algebra packages as used by Matlab. However, as the Givens rotations applied to (13) only act on the subsystem (14), we may use Householder reflections directly on (14). This allows to use standard Householder-based QR decompositions. Another possibility is a hardware-near implementation of the Givens rotation. For maintainability and readability reasons, we decided to use the standard linear algebra system as used by Matlab for the reference implementation.

If the sampling distances between adjacent data points d_i have very different orders of magnitude, so that the global mesh ratio $(\max_{i=1,\dots,N-1} d_i)/(\min_{i=1,\dots,N-1} d_i)$ is large, the matrix $A^{(r)}$, defined by (10), may have a large condition number. Then, solving (11) may get numerically unstable. In such cases, one may try data binning (meaning merging the data points with the smallest distances) to reduce the global mesh ratio.

2.4 Compatibility with pruning strategies

In the supplementary material, we show that the fast update strategy is compatible with the specific order of the computation of two different pruning strategies, the PELT strategy from Killick et al. (2012) and the pruning from Storath and Weinmann (2014), abbreviated here by FPVI. Comparing the two strategies, the effectiveness of FPVI essentially grows with the value of γ whereas the effectiveness of PELT essentially grows with the number of detected discontinuities.

2.5 Overall algorithm and computational effort

Putting together the procedures described in the last subsections, we obtain an algorithm which computes a solution \hat{J} of the minimization problem (3); that is, \hat{J} is a global minimizer of the target function in (3). Having computed the optimal discontinuity set \hat{J} , the corresponding CSSD \hat{f} is computed using the algorithm of Reinsch (1967). This completes the solution of (2). Altogether, we obtain:

Theorem 4. *The algorithm described above (sections 2.2 to 2.5) computes a solution of (2), i.e., a global minimizer of the target function in (2). The worst case time complexity is $O(N^2)$ and the memory complexity is $O(N)$.*

The proof is given in the supplementary material.

For details on the implementation, we refer to the provided reference implementation, cf. Section 3.1.

We point out that the scaling in runtime is often more favourable than the worst case scenario. This is an effect of the pruning strategies described in section 2.4. We observed in our experiments that the runtime scales approximately linearly if the number of detected discontinuities grows linearly with the signal's length. If there are no or very few detected discontinuities the runtime grows approximately quadratically. We refer to the experimental section for an illustrating example. Further, Killick et al. (2012) made similar observations for piecewise estimators and gave theoretical justifications for the PELT pruning strategy.

Remark 2. It is straightforward to extend the method to work for vector-valued data meaning that $y_i \in \mathbb{R}^D$ for all $i = 1, \dots, N$. In this case, $\mathcal{E}_{\{l:r\}}$ is simply the sum of the energies over all vector components $\sum_{j=1}^D \mathcal{E}_{\{l:r\},j}$, where $\mathcal{E}_{\{l:r\},j}$ is the spline energy of the j -th component of y on $\{l : r\}$. It is clear that the computational effort scales linearly with the dimension D .

2.6 Uniqueness result

As discussed in Section 2.2, the precise location of discontinuities between data sites does not influence the penalty function, so that a solution can only be unique up to shifts of discontinuities in between the data sites. Having reduced the potential discontinuities to midpoints (cf. Equation (6)), the optimal discontinuity set \hat{J} may still not be unique. A simple example is the data $x = [0, 1, 2]$ and $y = [0, 1, 0]$. For sufficiently small $\gamma > 0$, both $J = \{\frac{1}{2}\}$ and $\tilde{J} = \{\frac{3}{2}\}$ are optimal because they result in the same target functional value γ . A similar situation is found whenever the signal has odd length and has $\lceil N/2 \rceil - 1$ discontinuities. As it can be seen from the proof of Lemma 1, a solution with $\lceil N/2 \rceil - 1$ discontinuities is a piecewise linear function interpolating at most two data points. The ambiguities in the examples can be attributed to segments of length two or one, on which a smoothing spline acts interpolatory. If partitions with segments of length less than 3 can be ruled out, we obtain a uniqueness result for a.e. input $y \in \mathbb{R}^N$ (in a Lebesgue almost everywhere sense). The result is inspired by a related theorem of Wittich et al. (2008) on the piecewise constant model.

Theorem 5. *We consider the minimization problem (2) for the CSSD in its formulation (6) (with discontinuity set reduced to midpoints). Then, the minimizing values $f(x_i)$ at the data sites x_i are uniquely determined for a.e. input $y \in \mathbb{R}^N$ (w.r.t. Lebesgue measure.) Further, minimizing segments I^* of length at least three are uniquely determined for (Lebesgue-) a.e. input $y \in \mathbb{R}^N$. In particular, the minimizing function f is unique in $[x_{\min}, x_{\max}]$ where x_{\min}, x_{\max} denote the minimal and maximal argument value of the x_i in the minimizing segment I^* of length at least three. Consequently, minimizing partitions with all segments being of length at least three and corresponding minimizing functions (outside the intervals with the jumps) are uniquely determined for a.e. input $y \in \mathbb{R}^N$.*

The proof is given in the supplementary material.

In the present setup, a minimizer of (6) with at least 3 data sites between two discontinuities is obtained if γ is chosen sufficiently large. We note that one could also constrain the search space of (6) w.r.t. the size of the discontinuity sets as an alternative approach.

3 Experiments and parameter selection

3.1 Implementation and setup

The proposed algorithm was implemented in Matlab R2022b. For implementation details, we refer to the commented source code provided on Github². The numerical experiments were performed on a laptop with 2.4 GHz 8-Core Intel Core i9, 32 GB RAM. The choice of the model parameters p and γ depends on the sampling distances on the abscissa, on the scale of the data on the ordinate, and, of course, on the shape of the underlying signal. We set $\delta_i = \sigma$ for the synthetic experiments, where σ is the standard deviation of the noise, and $\delta_i = 1$ for the other experiments, for $i = 1, \dots, N$.

3.2 Simulated experiments with a manually selected parameter set.

As the proposed method is designed for estimating smoothly varying functions with discontinuities, we primarily choose test signals with these properties. A classical signal of this class is the “HeaviSine” function used in the work of Donoho and Johnstone (1994). It is given by $g_2(x) := 4 \sin(4\pi x) - \text{sign}(x - 0.3) - \text{sign}(0.72 - x)$. As second function of this class, we use the function $g_1(x) := J_1(20x) + x \cdot 1_{[0.3, 0.4]}(x) - x \cdot 1_{[0.6, 1]}(x)$ as test signal, where J_1 is the Bessel function of the first kind and 1_S is the indicator function on S . Compared to the HeaviSine, it has one discontinuity more and a varying amplitude. The discontinuity locations of g_1 are chosen such that g_1 shares one discontinuity with g_2 and such that the segments have different lengths. For the experiment shown in Figure 1 (in the introduction), we sampled the signal at $N = 100$ random points in the interval $[0, 1]$ (uniformly distributed) and corrupted them by additive zero mean Gaussian noise of standard deviation $\sigma = 0.1$. For a classical spline, a visually reasonable result was obtained using the parameter $p = 0.999$. Using this p -parameter, we report the results for several γ -values.

Experimental results for vector-valued input data are given in the supplementary material.

As the resulting function is a cubic spline with discontinuities it can be described by a piecewise cubic polynomial with discontinuities in J . Therefore, the result may serve as functional description of the discontinuous signal.

²Reference implementation of CSSD provided at <https://github.com/mstorath/CSSD>.

3.3 Computational costs

Next, we investigate the computational costs of the algorithm. As mentioned in the introduction, there is no freely available software package for solving (2) or its reduced form (6), to the authors knowledge. To assess the benefits of the proposed method, we implemented a baseline solver which relies on standard libraries for solving the reduced form (6). To this end, we combine a dynamic programming approach with the PELT-pruning strategy (Killick et al., 2012; Winkler and Liebscher, 2002), implemented in the Python module `ruptures`³ (Truong et al., 2020), for computing the optimal partition in (6). The necessary values of \mathcal{E}_l on each interval (cf. Equation (4)) were obtained as follows. The smoothing spline module `csaps`⁴, which is described as a Python replication of De Boor’s corresponding Fortran method, was used to compute a minimizer \hat{f}_l of (4) which in turn was used to compute \mathcal{E}_l using the corresponding equation given by De Boor (2001). As this baseline solver does not use the fast update scheme developed in this work, its worst case time complexity is $O(N^3)$ because the number of discrete intervals grows quadratically and the computational effort for a smoothing spline grows linearly in the interval length.

For the runtime comparison, we consider again the HeaviSine signal g_2 used in the last experiment, and we distinguish two experimental setups: In the first scenario, we increase the number of data points N by increasing the number of samples of the HeaviSine so that the number of discontinuities remains two. In the second scenario, we increase the number of data points by repeating the HeaviSine signal so that the number of discontinuities grows linearly with the signal length. We computed the CSSD for the parameters $p = 0.9999$ and $\gamma = 20$ which resulted in reasonably good estimates for the underlying true signal.

In Table 1, we report two measures of the computational effort, the runtimes and the frequency each data point is “visited” for computing all necessary $\mathcal{E}_{[l:r]}$. (The baseline algorithm needs the vector $y_{l:r}$ of length $r - l + 1$ while the proposed method only needs a single data point, y_l or y_r , depending on the order of update.)

We start our analysis by examining the frequencies at which each data point is visited. In the first scenario, where the number of discontinuities is held constant, the baseline method shows a pattern more akin to cubic growth, whereas the proposed method rather shows quadratic growth. For the second scenario, the growth in N trends towards linear for all considered methods. However, the hidden constant depends on the average segment length, and the relation is quadratic for the

³<https://github.com/deepcharles/ruptures>

⁴<https://github.com/espdev/csaps>

Signal length N	250	500	1000	2000	4000	8000
Constant number of discontinuities						
Baseline	$1.1 \cdot 10^6$	$2.7 \cdot 10^6$	$2.0 \cdot 10^7$	$1.5 \cdot 10^8$	$1.3 \cdot 10^9$	$7.3 \cdot 10^9$
	45.7	110.1	453.4	1909.1	8704.0	33331.3
Prop. + FPVI	$2.5 \cdot 10^4$	$10.0 \cdot 10^4$	$4.0 \cdot 10^5$	$1.7 \cdot 10^6$	$7.0 \cdot 10^6$	$2.9 \cdot 10^7$
	0.4	1.0	4.2	17.3	72.6	297.1
Prop. + PELT	$1.8 \cdot 10^4$	$4.3 \cdot 10^4$	$1.7 \cdot 10^5$	$6.8 \cdot 10^5$	$2.7 \cdot 10^6$	$9.5 \cdot 10^6$
	0.3	0.6	2.2	8.7	34.5	120.9
Increasing number of discontinuities						
Baseline	$3.9 \cdot 10^5$	$8.0 \cdot 10^5$	$7.4 \cdot 10^5$	$1.4 \cdot 10^6$	$2.9 \cdot 10^6$	$5.7 \cdot 10^6$
	28.6	57.8	81.8	158.9	323.6	652.3
Prop. + FPVI	$2.1 \cdot 10^4$	$9.1 \cdot 10^4$	$1.6 \cdot 10^5$	$2.4 \cdot 10^5$	$5.0 \cdot 10^5$	$1.3 \cdot 10^6$
	0.2	1.0	1.7	2.5	5.3	13.7
Prop. + PELT	$1.2 \cdot 10^4$	$2.4 \cdot 10^4$	$3.5 \cdot 10^4$	$6.9 \cdot 10^4$	$1.4 \cdot 10^5$	$2.8 \cdot 10^5$
	0.2	0.3	0.5	1.0	2.0	3.9

Table 1: Computational effort of the baseline solver and the proposed solver with different pruning strategies for computing a CSSD. The top rows represent the frequency a data item is visited by the algorithm, and the bottom rows the total runtime in seconds, respectively. The subtables show two scenarios: Increasing sampling density which results in a constant number of discontinuities, and repeating the signal so that the number of discontinuities scales linearly with the signal length. The reported values are averages over three runs with different noise realizations and a fixed parameter set.

baseline method, and linear for the proposed method. Importantly, in both scenarios, the proposed method significantly reduces computational effort with respect to the total frequencies at which each data point is visited.

We next look at the corresponding execution times. In the first scenario, we note that the corresponding runtimes for the baseline method exhibit a more favorable growth pattern compared to the growth pattern of the frequencies. This appears to be a consequence of the fact that the `csaps` function, which is used for computing the smoothing splines, shows a predominantly constant growth, and this diverges from the asymptotic linear growth for the majority of the sig-

nal lengths evaluated by the algorithm. An asymptotic cubic growth in runtime is expected for even longer signals than the ones currently used for comparison. Overall, the proposed method is much faster than the baseline method. In particular, the proposed methods allows to process signals of moderate size on a laptop repeatedly within a reasonable time frame.

In both scenarios of the above example, the PELT pruning is more effective than the FPVI pruning. Similar observations were made for other signals (not shown in this paper) in which the CSSD detects at least a few discontinuities. Interestingly, for the parameter selection by cross validation on the real data sets (Section 3.5) it is the other way round: the runtimes with FPVI pruning were 2.1 min (geyser data) and 5.8 h (stock data) whereas runtimes with PELT pruning were 2.7 min and 10.7 h, respectively. (A detailed table of the runtimes for each sampled (p, γ) value of the Geyser data is given in the supplementary material.) The reasons for the lower runtimes of FPVI pruning in these cases are that a relatively low number of discontinuities are detected and that the optimization procedure frequently evaluates the target functional for large values of γ where FPVI is more effective than PELT.

3.4 Automatic parameter selection

As for classical smoothing splines, it may be sufficient for some practical purposes to choose the model parameters by visual inspection; yet a procedure for automatic parameter selection is useful (cf. the discussion on this topic by Silverman (1985, Sec. 4)). To obtain an automatic proposal for the model parameters p and γ , we here use K -fold cross validation (CV) as follows. We partition the data randomly into K folds of approximately equal size. The K -fold cross validation score for p and γ is given by $\text{CV}(p, \gamma) = \frac{1}{N} \sum_{k=1}^K \sum_{i \in \text{Fold}_k} ((\hat{f}_{p,\gamma}^{-k}(x_i) - y_i)/\delta_i)^2$. Here, $\hat{f}_{p,\gamma}^{-k}$ denotes the result of the proposed algorithm applied to the all data except those in fold k . (Recall from Section 2.6 that the solutions of (2) might be non-unique. Yet, the proposed algorithm provides a unique solution, namely the one with the largest possible right-most interval, followed by the largest possible penultimate interval, and so on.) If an evaluation point x_i coincides with a discontinuity of $f_{p,\gamma}^{-k}$, we take the mean of the lefthand and the righthand limits: $f_{p,\gamma}^{-k}(x_i) = \lim_{t \rightarrow 0^+} \frac{1}{2}(f_{p,\gamma}^{-k}(x_i - t) + f_{p,\gamma}^{-k}(x_i + t))$. A typical choice is $K = 5$ folds (Hastie et al., 2009) which we adopt here. Optimal parameters p, γ in the sense of K -fold cross validation are minima of the scoring function $(p, \gamma) \mapsto \text{CV}(p, \gamma)$. To find a good parameter set in the sense of CV, we improve a starting value (p_0, γ_0)

using standard derivative-free optimizers: a global search via simulated annealing followed by a local refinement using the Nelder-Mead method. We use the implementations of Matlab with default options. The simulated annealing algorithm utilizes a balance of exploration (looking for new, possibly better solutions) and exploitation (optimizing around the best solution found so far), regulated by the temperature and its cooling schedule. By the mechanism of being able to escape local minima, it is less sensitive to the starting value than local methods. To save computation time, it is reasonable to use a starting value that gives a visually reasonable result based on the domain knowledge or prior experience. To enhance parallel processing, simulated annealing could be replaced by a grid search of the (p, γ) domain. For the optimization, γ is parametrized by $\gamma = p \frac{q}{1-q}$ with $q \in [0, 1)$. (This parametrization is obtained by dividing the functional by p and reparametrizing the resulting penalty $\gamma' = \gamma/p$ by $\gamma' = \frac{q}{1-q}$).

The procedure gives reasonable results in the conducted experiments (see results further below), but it comes with the limitations that the standard optimizers often need a high number of function evaluations leading to long runtimes, and that the resulting parameters are not guaranteed to be global minimizers of the CV scoring function. The second limitation can be mitigated by restarting the optimization with different starting values until no further improvement of the CV score is observed. As the costs for this improvement are additional computation time and/or manual refinement, we use this strategy only for the two real data experiments presented further below. For the synthetic example described further below, the initial values $p_0 = 0.99$ and $\gamma_0 = 1$ are used. (These parameters were chosen based on their ability to produce visually acceptable results for a set of sample signals.)

We compare the results of the proposed method to the following baseline method. We use the Bayesian ensemble method of Zhao et al. (2019), implemented in the toolbox `beast`⁵, to estimate changepoints and a corresponding piecewise estimate of the signal. To this end, the function `beast_irreg` (variant for nonuniform sample distances) is called with deactivated seasonality option (because the signal has no seasonality), time step option 0.01 (binning the non-equidistant samples to 100 bins of same length), and default parameters otherwise. (As internal preprocessing, `beast_irreg` aggregates data over bins of fixed width to obtain equidistant data sites. The procedure returns the first bin locations after the corresponding change; so to match the “midpoint convention” used in this paper, we work with the midpoint between the returned bin and the preceding

⁵Source code retrieved from <https://github.com/zhaokg/Rbeast> on Nov. 2, 2022.

non-empty bin.) We then fit a piecewise interpolating spline to the estimated values between the changepoints to obtain a functional estimate on the entire domain $[0, 1]$. (The interpolating spline is preferred over the smoothing spline here, because a smoothing spline would give different y -values at the data sites than those estimated by `beast` and would introduce an additional parameter.)

We use the experimental setup used for Figure 1 and two additional noise levels to compare the results of the two methods. Figure 3 shows the results for 100 signal realizations. We observe that the baseline method returns principally more changepoint candidates than the proposed method, and that a considerable portion of them are located away from the true discontinuity locations, e.g. near the local extrema of the test signal. The proposed method exhibits less spurious discontinuities than the baseline method and the cluster points in the histograms are more sharply located around the true discontinuity locations.

3.5 Results on real data using automatic parameter selection

The next experiment follows an example presented in the work of Silverman (1985) on smoothing splines. The data set contains the duration of eruptions along with the waiting time to the next eruption of the Old Faithful geyser in the Yellowstone National Park, USA; see Figure 4.⁶ When fitting a single straight line to the data, curvature effects in the residuals are observed. Silverman (1985) argues that fitting a smoothing spline is a useful exploratory step towards the choice of a reasonable model. Inspecting the shape of the resulting spline suggest a two phase linear regression model as plausible alternative. Remarkably, the CSSD model comprises both of the above models: The automatic parameter selection results in $\gamma = \infty$ so that the corresponding CSSD coincides with a classical smoothing spline. An appropriately chosen smaller γ -parameter gives a two phase model which is nearly linear on the two segments, and tends to a piecewise linear model for $p \rightarrow 0$. Ranking these three models by their CV scores, the classical spline can be considered as the best one, the linear model as the worst, and the two phase model lies in the middle. The example illustrates that the CSSD can serve as a useful tool for exploratory data analysis.

Eventually we report the results on a stock market time series. The present data shows the logarithm of the closing price of the Meta/Facebook stock from May 18,

⁶The data set was retrieved from the supplementary material of Wasserman (2004) <https://www.stat.cmu.edu/~larry/all-of-statistics/=data/faithful.dat>

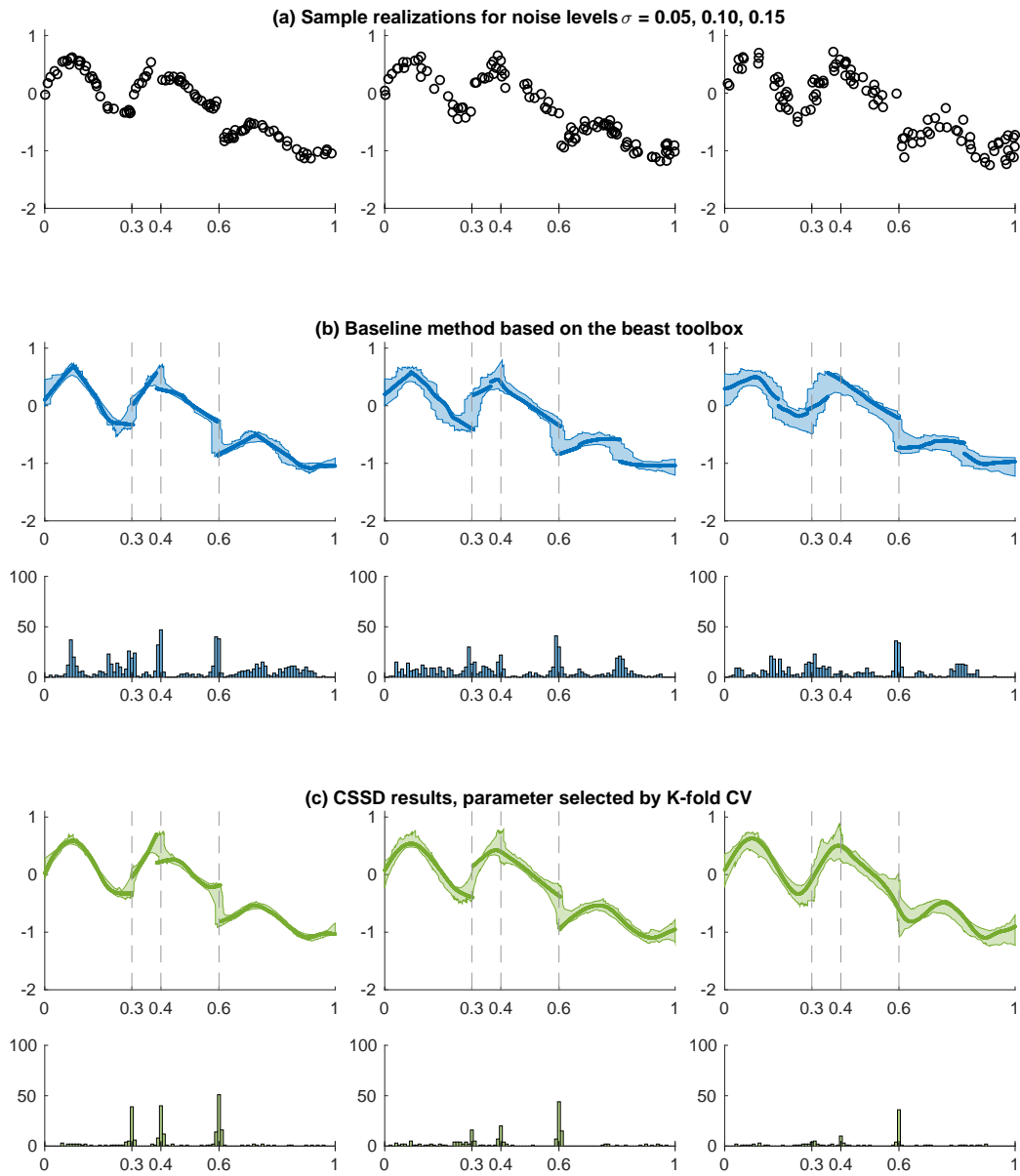


Figure 3: CSSD results with automatically selected parameter based on K-fold CV in comparison with a baseline method based on the beast toolbox. (a) Noisy samples of the test signal g_1 shown in Figure 1a with the noise levels $\sigma = 0.05, 0.1, 0.15$ (from left to right). (b) Results of the baseline method consisting of a method for piecewise regression with automatic parameter selection and subsequent spline interpolation. The dashed vertical lines indicate the true discontinuity locations. (As in Figure 1, the solid line represents the result for the sample signal, and the shaded regions represents the 2.5% to 97.5% quantiles, and the histograms represent the frequencies of the discontinuity locations.) (c) Results of the CSSD with automatic parameter selection based on K-fold cross validation.

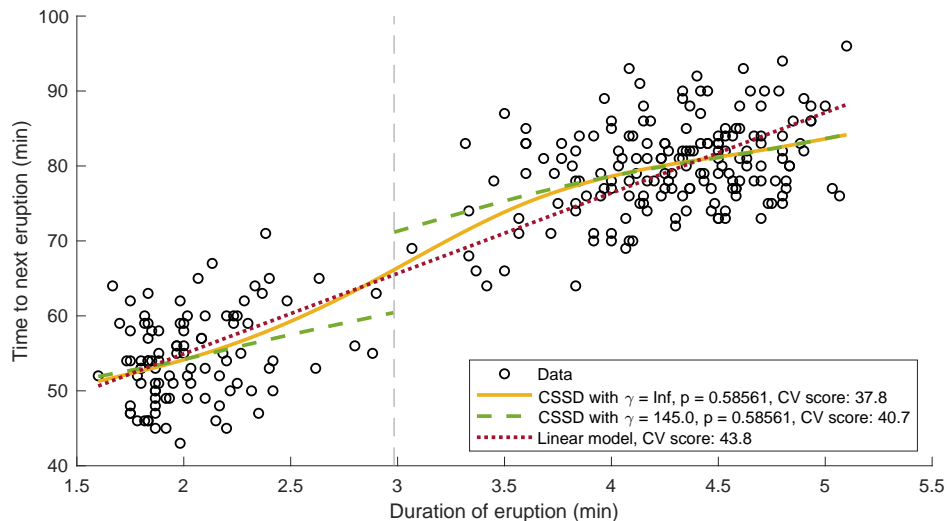


Figure 4: Fitting a CSSD to the Old Faithful data (circles): If the parameter is selected based on K-fold CV we obtain a result without discontinuities which coincides with a classical smoothing spline (solid curve). Keeping the selected p -parameter and lowering the γ parameter sufficiently gives a two-phase regression curve (dashed curves) with a breakpoint near $x = 3$ (dashed vertical line), and the two curve segments are nearly linear. Both of the above parameter sets yield better CV-scores than a linear model (dotted line).

2012, to May 19, 2022.⁷ The dates of the discontinuities can be related to strong market reactions after business reports: For example, on July 24, 2013, Facebook announced remarkable rises in revenues (Wilhelm, 2013). On July 25, 2018, Meta announced lower profit margins (Sharma and Vengattil, 2018), and on February 2, 2022, the price of Meta shares dropped strongly as Facebook reported a decline in daily users for the first time (Culliford and Balu, 2022). In this scenario, detected discontinuities could be interpreted as abrupt changepoints of the signal. The computation times are reported at the end of Section 3.3.

4 Conclusion and outlook

We have studied a variational model for cubic smoothing splines with unknown discontinuity locations which is a special case of the weak rod model. This model comprises classical continuous cubic splines (for sufficiently large γ parameters)

⁷Data source: <https://www.macrotrends.net/stocks/charts/FB/meta-platforms/stock-price-history>

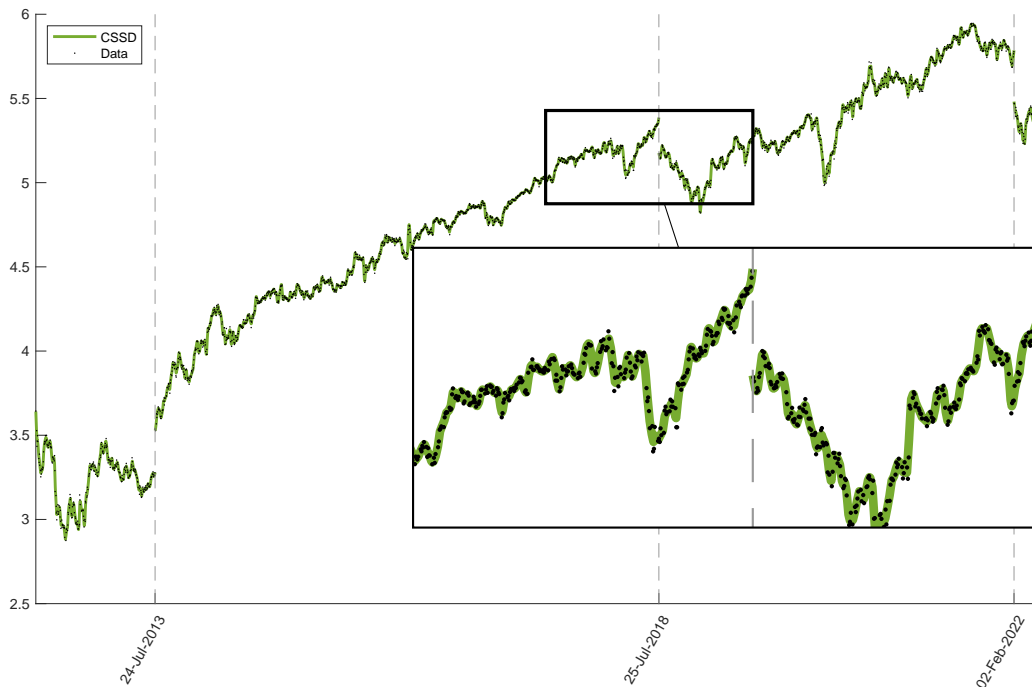


Figure 5: The dots represent the logarithm of the closing prices of the Meta stock from May 18, 2012, to May 19, 2022. The curve represents the CSSD with parameters determined by K-fold CV ($p = 0.4702$, $\gamma = 0.0069$). The dashed vertical lines indicate the discontinuities of the CSSD, and the ticks correspond to the date before the discontinuity.

and piecewise linear regression (for $p \rightarrow 0$). We have shown that the solutions are unique in an almost everywhere sense on segments comprising at least three data sites. We developed an efficient algorithm for computing the global minimizer of the model’s underlying optimization problem. The runtime experiments indicated that the method is particularly efficient for signals with many discontinuities. But also in the general case, the algorithm can be executed on a laptop in reasonable time for signals of moderate lengths. The algorithm is applicable to data with non-equidistant sampling points and to vector-valued data. Automatic parameter selection based on K-fold cross validation gave reasonable results for synthetic and real data; the main limitation of this selection strategy is currently the relatively high runtime. The numerical examples have illustrated potential applications of a CSSD: as function estimator for a discontinuous signal, as basis for a changepoint detector, or as tool for exploratory data analysis.

Open questions for future work include faster algorithms for automatically

selecting the model parameters, extension to splines of higher orders and higher dimensions, and further investigation of theoretical properties of the estimator.

Supplementary Material

Supplementary document: The supplementary document contains proofs of the theorems, justifications for the compatibility with the pruning strategies, and additional experiments.

Acknowledgement

MS was supported by the research program “Informations- und Kommunikationstechnik” of the Bavarian State Ministry of Economic Affairs, Regional Development and Energy (DIK-2105-0044 / DIK0264). AW acknowledges support of Deutsche Forschungsgemeinschaft (DFG) under project number 514177753. The authors report there are no competing interests to declare.

References

- S. Arlot and A. Celisse. Segmentation of the mean of heteroscedastic data via cross-validation. *Statistics and Computing*, 21(4):613–632, 2011.
- I. E. Auger and C. E. Lawrence. Algorithms for the optimal identification of segment neighborhoods. *Bulletin of Mathematical Biology*, 51(1):39–54, 1989.
- R. Baranowski, Y. Chen, and P. Fryzlewicz. Narrowest-over-threshold detection of multiple change points and change-point-like features. *Journal of the Royal Statistical Society. Series B: Statistical Methodology*, 81(3):649–672, 2019.
- A. Blake and A. Zisserman. *Visual reconstruction*. MIT Press Cambridge, 1987.
- A. Blake. Comparison of the efficiency of deterministic and stochastic algorithms for visual reconstruction. *IEEE Transactions on Pattern Analysis and Machine Intelligence*, 11(1):2–12, 1989.
- L. Boysen, A. Kempe, V. Liebscher, A. Munk, and O. Wittich. Consistencies and rates of convergence of jump-penalized least squares estimators. *The Annals of Statistics*, 37(1):157–183, 2009.
- E. Cheney. *Introduction to approximation theory*. 1998. reprint of the 2nd de(1982) edn.
- P. Craven and G. Wahba. Smoothing noisy data with spline functions: estimating the correct degree of smoothing by the method of generalized cross-validation. *Numerische Mathematik*, 31(4):377–403, 1979.

- E. Culliford and N. Balu. Meta shares sink 20% as Facebook loses daily users for the first time. *Reuters*, 2022. URL <https://www.reuters.com/technology/facebook-owner-meta-forecasts-q1-revenue-below-estimates-2022-02-02/>.
- C. De Boor. *A practical guide to splines - Revised Edition*, volume 27. Springer-Verlag New York, 2001.
- F. De Hoog and M. Hutchinson. An efficient method for calculating smoothing splines using orthogonal transformations. *Numerische Mathematik*, 50(3):311–319, 1986.
- D. L. Donoho and J. M. Johnstone. Ideal spatial adaptation by wavelet shrinkage. *Biometrika*, 81(3):425–455, 1994.
- R. L. Dougherty, A. S. Edelman, and J. M. Hyman. Nonnegativity-, monotonicity-, or convexity-preserving cubic and quintic Hermite interpolation. *Mathematics of Computation*, 52(186):471–494, 1989.
- A. Drobyshev, C. Machka, M. Horsch, M. Selmann, V. Liebscher, M. de Angelis, and J. Beckers. Specificity assessment from fractionation experiments (safe): a novel method to evaluate microarray probe specificity based on hybridisation stringencies. *Nucleic acids research*, 31(2):1–10, 2003.
- P. Fearnhead. Exact and efficient Bayesian inference for multiple changepoint problems. *Statistics and computing*, 16(2):203–213, 2006.
- K. Frick, A. Munk, and H. Sieling. Multiscale change point inference. *Journal of the Royal Statistical Society: Series B (Statistical Methodology)*, 76(3):495–580, 2014.
- F. Friedrich, A. Kempe, V. Liebscher, and G. Winkler. Complexity penalized M-estimation. *Journal of Computational and Graphical Statistics*, 17(1):201–224, 2008.
- P. Fryzlewicz. Wild binary segmentation for multiple change-point detection. *The Annals of Statistics*, 42(6):2243–2281, 2014.
- G. H. Golub, M. Heath, and G. Wahba. Generalized cross-validation as a method for choosing a good ridge parameter. *Technometrics*, 21(2):215–223, 1979.
- P. J. Green and B. W. Silverman. *Nonparametric regression and generalized linear models: a roughness penalty approach*. CRC Press, 1993.
- T. Hastie, R. Tibshirani, J. H. Friedman, and J. H. Friedman. *The elements of statistical learning: data mining, inference, and prediction*, volume 2. Springer, 2009.
- K. Haynes, P. Fearnhead, and I. A. Eckley. A computationally efficient nonparametric approach for changepoint detection. *Statistics and computing*, 27:1293–1305, 2017.
- T. Hotz, O. M. Schutte, H. Sieling, T. Polupanow, U. Diederichsen, C. Steinem, and A. Munk. Idealizing ion channel recordings by a jump segmentation multiresolution filter. *IEEE Transactions on NanoBioscience*, 12(4):376–386, 2013.
- P. Hupé, N. Stransky, J. Thiery, F. Radvanyi, and E. Barillot. Analysis of array CGH data: from signal ratio to gain and loss of DNA regions. *Bioinformatics*, 20(18):3413–3422, 2004.
- M. Hutchinson. Algorithm 642: A fast procedure for calculating minimum cross-validation cubic smoothing splines. *ACM Transactions on Mathematical Software (TOMS)*, 12(2):150–153, 1986.
- B. Jackson, J. D. Scargle, D. Barnes, S. Arabhi, A. Alt, P. Gioumouisis, E. Gwin, P. Sangtrakulcharoen, L. Tan, and T. T. Tsai. An algorithm for optimal partitioning of data on an

- interval. *IEEE Signal Processing Letters*, 12(2):105–108, 2005.
- S. Jeong, T. Park, and D. A. van Dyk. Bayesian model selection in additive partial linear models via locally adaptive splines. *Journal of Computational and Graphical Statistics*, pages 1–13, 2021.
- C. Joo, H. Balci, Y. Ishitsuka, C. Buranachai, and T. Ha. Advances in single-molecule fluorescence methods for molecular biology. *Annu. Rev. Biochem.*, 77:51–76, 2008.
- R. Killick, P. Fearnhead, and I. Eckley. Optimal detection of changepoints with a linear computational cost. *Journal of the American Statistical Association*, 107(500):1590–1598, 2012.
- K.-R. Kim, I. L. Dryden, H. Le, and K. E. Severn. Smoothing splines on Riemannian manifolds, with applications to 3d shape space. *Journal of the Royal Statistical Society: Series B (Statistical Methodology)*, 83(1):108–132, 2021.
- J. Kleinberg and É. Tardos. *Algorithm design*. Pearson Education India, 2006.
- J.-Y. Koo. Spline estimation of discontinuous regression functions. *Journal of Computational and Graphical Statistics*, 6(3):266–284, 1997.
- M. A. Little and N. S. Jones. Generalized methods and solvers for noise removal from piecewise constant signals. I. Background theory. *Proceedings of the Royal Society A: Mathematical, Physical and Engineering Science*, 467(2135):3088–3114, 2011a.
- M. A. Little and N. S. Jones. Generalized methods and solvers for noise removal from piecewise constant signals. II. New methods. *Proceedings of the Royal Society A: Mathematical, Physical and Engineering Science*, 467(2135):3115–3140, 2011b.
- L. Loeff, J. W. Kerssemakers, C. Joo, and C. Dekker. Autostepfinder: A fast and automated step detection method for single-molecule analysis. *Patterns*, 2(5):100256, 2021.
- S. Mallat. *A wavelet tour of signal processing: the sparse way*. Academic press, 2008.
- C. Meng, J. Yu, Y. Chen, W. Zhong, and P. Ma. Smoothing splines approximation using Hilbert curve basis selection. *Journal of Computational and Graphical Statistics*, pages 1–11, 2022.
- D. Mumford and J. Shah. Boundary detection by minimizing functionals. In *IEEE Conference on Computer Vision and Pattern Recognition*, volume 17, pages 137–154, 1985.
- D. Mumford and J. Shah. Optimal approximations by piecewise smooth functions and associated variational problems. *Communications on Pure and Applied Mathematics*, 42(5):577–685, 1989.
- E. S. Page. Continuous inspection schemes. *Biometrika*, 41(1/2):100–115, 1954.
- C. H. Reinsch. Smoothing by spline functions. *Numerische Mathematik*, 10(3):177–183, 1967.
- I. Schoenberg. On best approximations of linear operators. In *Nederl. Akad. Wetensch. Proc. Ser. A*, volume 67, pages 155–163, 1964a.
- I. J. Schoenberg. Spline functions and the problem of graduation. *Proc. Amer. Math. Soc.*, 52: 947–950, 1964b.
- V. Sharma and M. Vengattil. Zuckerberg loses more than \$15 billion in record Facebook fall. *Reuters*, 2018. URL <https://www.reuters.com/article/us-facebook-results-stock-idUSKBN1KG1TN>.
- B. W. Silverman. Spline smoothing: the equivalent variable kernel method. *The Annals of Statistics*, pages 898–916, 1984.

- B. W. Silverman. Some aspects of the spline smoothing approach to non-parametric regression curve fitting. *Journal of the Royal Statistical Society: Series B (Methodological)*, 47(1):1–21, 1985.
- A. Snijders, N. Nowak, R. Segreaves, et al. Assembly of microarrays for genome-wide measurement of DNA copy number by CGH. *Nature genetics*, 29:263–264, 2001.
- Y. Sowa, A. Rowe, M. Leake, T. Yakushi, M. Homma, A. Ishijima, and R. Berry. Direct observation of steps in rotation of the bacterial flagellar motor. *Nature*, 437(7060):916–919, 2005.
- M. Storath and A. Weinmann. Fast partitioning of vector-valued images. *SIAM Journal on Imaging Sciences*, 7(3):1826–1852, 2014.
- M. Storath, A. Weinmann, and L. Demaret. Jump-sparse and sparse recovery using Potts functionals. *IEEE Transactions on Signal Processing*, 62(14):3654–3666, 2014.
- M. Storath, A. Weinmann, and M. Unser. Jump-penalized least absolute values estimation of scalar or circle-valued signals. *Information and Inference: A Journal of the IMA*, 6(3):225–245, 2017.
- M. Storath, L. Kiefer, and A. Weinmann. Smoothing for signals with discontinuities using higher order Mumford-Shah models. *Numerische Mathematik*, 143(2):423–460, 2019.
- S. O. Tickle, I. Eckley, P. Fearnhead, and K. Haynes. Parallelization of a common changepoint detection method. *Journal of Computational and Graphical Statistics*, 29(1):149–161, 2020.
- C. Truong, L. Oudre, and N. Vayatis. Selective review of offline change point detection methods. *Signal Processing*, 167:107299, 2020.
- M. Unser. Splines: A perfect fit for signal and image processing. *IEEE Signal Processing Magazine*, 16(6):22–38, 1999.
- M. Unser. Splines: a perfect fit for medical imaging. In *Medical Imaging 2002: Image Processing*, volume 4684, pages 225–236. International Society for Optics and Photonics, 2002.
- G. J. J. van den Burg and C. K. I. Williams. An evaluation of change point detection algorithms. 2020. URL <https://arxiv.org/abs/2003.06222>.
- G. Wahba. *Spline models for observational data*. SIAM, 1990.
- L. Wasserman. *All of Statistics – A Concise Course in Statistical Inference*. Springer, 2004.
- A. Weinmann and M. Storath. Iterative Potts and Blake-Zisserman minimization for the recovery of functions with discontinuities from indirect measurements. *Proceedings of the Royal Society A: Mathematical, Physical and Engineering Sciences*, 471(2176):20140638, 2015.
- A. Weinmann, M. Storath, and L. Demaret. The L^1 -Potts functional for robust jump-sparse reconstruction. *SIAM Journal on Numerical Analysis*, 53(1):644–673, 2015.
- A. Weinmann, L. Demaret, and M. Storath. Mumford-Shah and Potts regularization for manifold-valued data. *Journal of Mathematical Imaging and Vision*, 55(3):428–445, 2016.
- E. T. Whittaker. On a new method of graduation. *Proceedings of the Edinburgh Mathematical Society*, 41:63–75, 1923.
- A. Wilhelm. Facebook q2 earnings beat expectations with \$1.81b in revenue, up 53%, mobile hits 41% of ad revenue. *Techcrunch*, 2013. URL <https://techcrunch.com/2013/07/24/facebook-q2-earnings-beats-with-1-81b-in-revenue-up-53-mobile-hits-41-of-ad-revenue/>.
- G. Winkler and V. Liescher. Smoothers for discontinuous signals. *Journal of Nonparametric Statistics*, 14(1-2):203–222, 2002.

- G. Winkler, O. Wittich, V. Liebscher, and A. Kempe. Don't shed tears over breaks. *Jahresbericht DMV*, 107:57–87, 2005.
- G. Winkler. *Image analysis, random fields and Markov chain Monte Carlo methods: a mathematical introduction*, volume 27. Springer Science & Business Media, 2003.
- O. Wittich, A. Kempe, G. Winkler, and V. Liebscher. Complexity penalized least squares estimators: Analytical results. *Mathematische Nachrichten*, 281(4):582–595, 2008.
- G. Yang, B. Zhang, and M. Zhang. Estimation of knots in linear spline models. *Journal of the American Statistical Association*, pages 1–12, 2021.
- Y.-C. Yao. Estimating the number of change-points via Schwarz' criterion. *Statistics & Probability Letters*, 6(3):181–189, 1988.
- N. R. Zhang and D. O. Siegmund. A modified Bayes information criterion with applications to the analysis of comparative genomic hybridization data. *Biometrics*, 63(1):22–32, 2007.
- K. Zhao, M. A. Wulder, T. Hu, R. Bright, Q. Wu, H. Qin, Y. Li, E. Toman, B. Mallick, X. Zhang, et al. Detecting change-point, trend, and seasonality in satellite time series data to track abrupt changes and nonlinear dynamics: A Bayesian ensemble algorithm. *Remote Sensing of Environment*, 232:111181, 2019.
- C. Zou, G. Yin, L. Feng, and Z. Wang. Nonparametric maximum likelihood approach to multiple change-point problems. *The Annals of Statistics*, 42(3):970–1002, 2014. URL <https://doi.org/10.1214/14-AOS1210>.

A Supplementary document for “Smoothing splines for discontinuous signals”

This is supplementary material for the paper: Martin Storath, Andreas Weinmann, “Smoothing splines for discontinuous signals”. The equations, statements and references refer to the corresponding elements in the main document.

A.1 Proofs

A.1.1 Proof of Lemma 1

Proof. 1. Let J be a minimizer of (2). Assume that J has two elements j_1, j_2 , with $j_1 < j_2$, between two adjacent data sites x_i, x_{i+1} . Let f_j be the corresponding optimal function. By a basic property of cubic smoothing splines (see e.g. (Silverman, 1985)), f_j is an affine linear function on $[x_i, j_1)$. This affine linear function can be extended to $[j_1, j_2)$. The extension does not increase the roughness penalty, and decreases the discontinuity penalty by $\gamma > 0$. Hence, J was not a minimizer. For more than two discontinuities, the above argument is applied repeatedly.

2. For data of length N , we find a discontinuity set J of size $\lceil N/2 \rceil - 1$ which partitions $[x_1, x_N]$ into $\lceil N/2 \rceil$ segments containing at most two data sites each. On each of the segments, the optimal spline is a linear function connecting the two data points (or a constant function if the segment contains only one point) so that both the data penalty and the roughness penalty become 0. Thus, the only remaining penalty is the discontinuity penalty which is equal to $\gamma J = \gamma(\lceil N/2 \rceil - 1)$. This shows that the minimum functional value of (2) is bounded from above by $\gamma(\lceil N/2 \rceil - 1)$. Now if $|\hat{J}| > (\lceil N/2 \rceil - 1)$, the functional value is strictly larger than $\gamma(\lceil N/2 \rceil - 1)$ which is a contradiction. \square

A.1.2 Proof of Lemma 2

Proof. Denote the functional in (4), with $I = \{1 : r\}$, by $L_1(f)$ (defined for arguments $f \in C^2([x_1, x_r])$), and denote the functional in (11) by $L_2(u)$ (defined for arguments $u \in \mathbb{R}^{2r}$).

Let \hat{f} be the minimizer of L_1 , and let $\hat{v} \in \mathbb{R}^{2r}$ such that $\hat{v}_{2i-1} = \hat{f}(x_i)$ and $\hat{v}_{2i} = \hat{f}'(x_i)$ for all $i = 1, \dots, r$. In the derivation before Lemma 2 (equations (8) to (10)) we constructed $A^{(r)}$ and $\tilde{y}^{(r)}$ such that $\mathcal{E}_{\{1:r\}} = L_2(\hat{v})$. This implies that

$$\mathcal{E}_{\{1:r\}} = L_2(\hat{v}) \geq \min_{u \in \mathbb{R}^{2r}} L_2(u) = L_2(\hat{u}). \quad (16)$$

where $\hat{u} \in \mathbb{R}^{2r}$ is the minimizer of L_2 .

Let H be the unique piecewise cubic polynomial described by \hat{u} , i.e. $H(x_i) = \hat{u}_{2i-1}$ and $H'(x_i) = \hat{u}_{2i}$. By construction H is a piecewise cubic polynomial and $H \in C^1([x_1, x_r])$. Let S be the interpolating cubic spline of the points $(x_i, H(x_i))$ for $i = 1, \dots, r$ with natural boundary conditions. Since $H(x_i) = S(x_i)$ for all $i = 1, \dots, r$, H and S have the same data deviation penalty (the first term in (4)). Towards a contradiction, assume that $H \neq S$ on $[x_1, x_r]$. H' is absolutely continuous, because it is continuous and differentiable up to a finite set. Thus H' is differentiable in the sense of Lebesgue, and $H'' \in L^2([x_1, x_r])$, because H'' is piecewise continuous with only step discontinuities at the data sites. Because $H \neq S$ by assumption, we get by the second minimality property of splines (Schoenberg, 1964a) that

$$\int_{x_1}^{x_r} (H''(x))^2 dx > \int_{x_1}^{x_r} (S''(x))^2 dx.$$

Therefore, we get for $v \in \mathbb{R}^{2r}$ with $v_{2i-1} = S(x_i)$ and $v_{2i} = S'(x_i)$ that $L_2(v) < L_2(\hat{u})$ which contradicts the optimality of \hat{u} . Hence, $H = S$. It follows that

$$L_2(\hat{u}) = L_1(H) = L_1(S) \geq \min_{f \in \mathcal{C}^2([x_1, x_r])} L_1(f) = \mathcal{E}_{\{1:r\}}. \quad (17)$$

Combining (16) and (17) we get $L_2(\hat{u}) \geq \mathcal{E}_{\{1:r\}} \geq L_2(\hat{u})$ which completes the proof. \square

A.1.3 Proof of Theorem 3

Proof. The validity of the update scheme (15) follows directly from the derivation described between (12) and (15). It remains to prove the statement on the complexity. The update (15) needs only a constant number of Givens rotations which act on submatrix of size 5×4 . Thus, the computational cost for an update step (15) is constant, $O(1)$, and so computing the entire vector $[\mathcal{E}_{\{1:1\}}, \mathcal{E}_{\{1:2\}}, \dots, \mathcal{E}_{\{1:N\}}]$ is $O(N)$. The memory complexity is $O(N)$ because the matrices $A^{(N)}$ is a band-matrix which retains its band-structure after application of the Givens rotations. \square

A.1.4 Proof of Theorem 4

Proof. We have seen in Section 2.2 that a solution of (2) can be obtained by solving (6) which in turn can be solved by computing F_r^* for $r = 1, \dots, N$, by (7) or its pruned version (24). It remains to show the assertions on the complexity. By Theorem 3, computation of $\mathcal{E}_{\{l:r\}}$ for all $l = 1, \dots, r$ is $O(r)$ time and memory, so

computing F_r^* is $O(r)$ time and memory, provided that F_l^* has been stored for $l = 1, \dots, r - 1$. Hence, computing the final minimum F_N^* is at most $O(N^2)$ time. The final CSSD is computed via determining the minimizing argument of (4) between two discontinuity locations. This can be done using Reinsch's algorithm which is in total $O(N)$ time and $O(N)$ memory, see Reinsch (1967) and De Boor (2001). Storing the F^* values needs $O(N)$ memory, and storing the optimal discontinuity locations is $O(N)$ memory as well. The values $\mathcal{E}_{\{l:r\}}$, $l = 1, \dots, r$, can be discarded once F_r^* has been determined. Hence, the overall memory complexity is $O(N)$. \square

A.1.5 Proof of Theorem 5

Proof. (1) For convenience, we first formulate the functionals in (6) with an explicit dependence on the data $y \in \mathbb{R}^N$:

$$\mathcal{G}(J, y) = \sum_{I \in \mathcal{P}(J)} \mathcal{E}_{I,y} + \gamma|J|,$$

where $\mathcal{E}_{I,y}$ is given by (4), i.e.,

$$\mathcal{E}_{I,y} = \min_{f \in \mathcal{C}^2(I)} p \sum_{i: x_i \in I} \left(\frac{y_i - f(x_i)}{\delta_i} \right)^2 + (1 - p) \int_I (f''(t))^2 dt.$$

For any interval I , the minimizer of (4) is the corresponding smoothing spline f_I^* which is uniquely determined; cf. e.g. De Boor (2001). Hence, the mapping from data y_I on (a discrete subset of) the interval I to the corresponding smoothing spline on I is well defined. We denote the mapping restricted to data sites in I by

$$S_I(y_I) := f_I^*|_{x_1, \dots, x_N}.$$

The smoothing spline solution operator S_I is a linear mapping acting on a linear space of dimension $d_I := \#\{x_i : x_i \in I\}$, the number of data sites in I . If and only if $d_I = 2$, S_I equals the identity E , thus

$$S_I - E = 0 \quad \Leftrightarrow \quad d_I = 2.$$

Given a (centered midpoint) jump set J with corresponding partitioning $\mathcal{P}(J)$ we consider the corresponding block diagonal matrix

$$S_{\mathcal{P}(J)} = \begin{bmatrix} S_{I_1} & 0 & \cdots & 0 \\ 0 & S_{I_2} & \cdots & 0 \\ \vdots & \ddots & \ddots & \vdots \\ 0 & \cdots & 0 & S_{I_k} \end{bmatrix} \quad (18)$$

where each $I \in \mathcal{P}(J)$ corresponds to a diagonal block containing the (matrix representation) of the spline solution operator S_I . Here k denotes the number of parts in $\mathcal{P}(J)$. $S_{\mathcal{P}(J)}$ represents the solution operator of (6) for any given J . We make the straight-forward but important observation that, for (centered midpoint) jump sets J, J'

$$S_{\mathcal{P}(J)} = S_{\mathcal{P}(J')} \quad \Leftrightarrow \quad \text{For all } I \in \mathcal{P}(J) \text{ with } d_I > 2, I \in \mathcal{P}(J'), \quad (19)$$

i.e., those segments of the corresponding partitions which have length at least three need to belong to both partitions. This leads to the following nomenclature: We call two (midpoint) jump sets J, J' or partitions $\mathcal{P}, \mathcal{P}'$ *essentially different*, if their corresponding matrices $S_{\mathcal{P}(J)}$ are not equal.

(2) Next, we aim at showing that for two essentially different jump sets J, J' we have

$$\mathcal{N}(J, J') = \{y \in \mathbb{R}^N : \mathcal{G}(J, y) = \mathcal{G}(J', y)\} \quad (20)$$

has Lebesgue measure zero. Actually, we show that the Lebesgue measure of the level sets

$$L_{J,c} = \{y \in \mathbb{R}^N : \mathcal{G}(J, y) = c\}, \quad c \in \mathbb{R}, \quad (21)$$

equals 0 which in turn implies (20). To this end we plug in the smoothing spline solution operator $S_{\mathcal{P}(J)}$ to get

$$\mathcal{E}_{I,y} = p \sum_{i: x_i \in I} \left(\frac{y_i - S_I y(x_i)}{\delta_i} \right)^2 + (1-p) \int_I (S_I y''(t))^2 dt. \quad (22)$$

Please note that by a slight abuse of notation we also use the symbol S_I to denote the smoothing spline operator (without sampling at the data sites) here. (The related identification mapping is given by spline interpolation.) If $d_I \leq 2$, $\mathcal{E}_{I,y}$ equals 0 for all data y . It is well-known (cf. De Boor (2001)) that the integral on the right-hand side can be written as a quadratic functional in the data y , i.e.,

$$\int_I (S_I y''(t))^2 dt = y^T A y = y^T \Delta^T K \Delta y, \quad (23)$$

with a symmetric square matrix A of dimension d_I , a second difference matrix Δ and an invertible square matrix K of dimension $d_I - 2$. (Details may be found for instance in De Boor (2001).) The kernel of Δ , and thus A equals the subspace of affine-linear functions, or more precisely, samples thereof. The gradient of the quadratic form $y \mapsto y^T A y$ equals $2\Delta^T K \Delta y$ which is non-zero whenever y does not equal (the sample of) an affine linear function. Hence, choosing a complement of

the two-dimensional subspace of affine-linear functions, the corresponding level sets $\{y : y^T A y = \text{const}\}$ are Lebesgue zero sets. In turn, $\{y \in \mathbb{R}^{d_t} : y^T A y = \text{const}\}$ as well as $\{y \in \mathbb{R}^{d_t} : \mathcal{G}(J, y) = \text{const}\}$ are Lebesgue zero sets. This shows (21), and in consequence (20).

(3) Now we may use the statement of (20) to show the assertions of Theorem 5. We first show that the minimizing values $f(x_i)$ at the data sites x_i are uniquely determined for a.e. input $y \in \mathbb{R}^N$. To see this, we exclude those $y' \in \mathbb{R}^N$ for which there are at least two essentially different J, J' such that $y \in \mathcal{N}(J, J')$. Let us call this exclusion set Y' . Since all $\mathcal{N}(J, J')$ are sets of Lebesgue measure zero and there are only finitely many different midpoint jump sets, the corresponding union w.r.t. J, J' is a set of Lebesgue measure zero as well. Hence, Y' is a zero set, and on its complement the minimizing essential partition is unique. Next, we show that minimizing segments I^* of size at least three are uniquely determined for a.e. $y \in \mathbb{R}^N$. To this end, we exclude the same zero set Y' as above. On the complement of Y' , the essential minimizing jump set is unique. Further, for any two J, J' with $S_{\mathcal{P}(J)} = S_{\mathcal{P}(J')}$ (equivalent jump sets), both corresponding partitions need to contain the same intervals of size larger than two by (19). Thus, they are uniquely determined on Y' . Consequently, by the uniqueness of the smoothing spline, the minimizing function f is unique in $[x_{\min}, x_{\max}]$ where x_{\min}, x_{\max} denote the minimal and maximal argument value of the x_i in the minimizing segment I^* of length at least three. If all segments are of length at least three, for any two J, J' with $S_{\mathcal{P}(J)} = S_{\mathcal{P}(J')}$ implies $J = J'$ (midpoint centered jump sets.) Hence, a corresponding jump set J uniquely represents its matrix in $S_{\mathcal{P}(J)}$ in (18) (actually its equivalence class). In consequence, on Y' , the segments taking the minimal value in (6) unique. The corresponding statement for the function f is again a consequence of the uniqueness of the smoothing spline. Together, this shows all assertions of the theorem and completes the proof. \square

A.2 Compatibility with pruning strategies

To use the FPVI pruning, we reformulate (7) as follows:

$$F_r^* = \min \left\{ \mathcal{E}_{\{1:r\}}; \min_{l=r-1, r-2, \dots, 2} \mathcal{E}_{\{l:r\}} + \gamma + F_{l-1}^* \right\}. \quad (24)$$

The first term in the parenthesis captures the cost of using a classical spline on the entire interval. The second term captures the cost of concatenating a continuous spline on $\{l : r\}$ with the already computed optimal discontinuous spline on $\{1 : l-1\}$. We compute F_r^* as follows. We define $F_{r,r}^* := \mathcal{E}_{\{1:r\}}$ and sequentially compute, for $l = r-1, r-2, \dots, 2$,

$$F_{l,r}^* = \min \left\{ F_{l+1,r}^*; \mathcal{E}_{\{l:r\}} + \gamma + F_{l-1}^* \right\}. \quad (25)$$

Then, $F_r^* = F_{2,r}^*$. We observe that $F_l^* \geq 0$ for all $l = 1, \dots, r$ and $\mathcal{E}_{\{l:r\}}$ is non-decreasing for the reverse order $l = r-1, r-2, \dots, 2$. Thus, if

$$\mathcal{E}_{\{l:r\}} + \gamma \geq F_{l,r}^*, \quad (26)$$

we obtain, for all $l' \leq l$,

$$F_{l,r}^* \leq \mathcal{E}_{\{l:r\}} + \gamma \leq \mathcal{E}_{\{l':r\}} + \gamma \leq \mathcal{E}_{\{l':r\}} + \gamma + F_{l'}^* \leq F_{l',r}^*.$$

So when condition (26) is fulfilled we may break the l -loop and set $F_r^* = F_{l,r}^*$.

It remains to show that the pruning is compatible with the order of computation of the $\mathcal{E}_{l,r}$. This can be seen as follows: The first term in parenthesis $\mathcal{E}_{\{1:r\}}$ of (24) is precomputed for $r = 1, \dots, N$, in that order. By Theorem 3, this requires linear time and memory, and thus is uncritical for the overall complexity. To use the computation scheme (25), we need to compute the $\mathcal{E}_{\{l:r\}}$ in reverse order, meaning in the order $l = r-1, r-2, \dots, 2$. But this can simply be achieved by applying the update scheme on the flipped data vector.

When using the PELT pruning, the minimum in (7) has to be sought over an active set of left bounds \mathcal{A}_r , so $F_r^* = \min_{l \in \mathcal{A}_r} \left\{ \mathcal{E}_{\{l:r\}} + \gamma + F_{l-1}^* \right\}$. After step r , the active set is pruned according to $\mathcal{A}_{r+1} = \{l \in \mathcal{A}_r \cup \{r\} : F_{l-1}^* + \mathcal{E}_{\{l:r\}} \leq F_r^*\}$. As $\mathcal{A}_{r+1} \subset \mathcal{A}_r \cup \{r\}$, we may compute the splines energies in the update order $\mathcal{E}_{\{l,r\}} \rightarrow \mathcal{E}_{\{l,r+1\}}$ for all active left bounds $l \in \mathcal{A}_{r+1}$ with $l < r$; and if $l = r$ we start a new recursion by computing the initial state corresponding to $\mathcal{E}_{\{r:r+1\}}$. As for FPVI, the case with no discontinuities can be handled by initializing $F_r^* = \mathcal{E}_{\{1:r\}}$ for all $r = 1, \dots, N$, so that the recursion can be started with $r = 3$ and $\mathcal{A}_3 = \{2\}$.

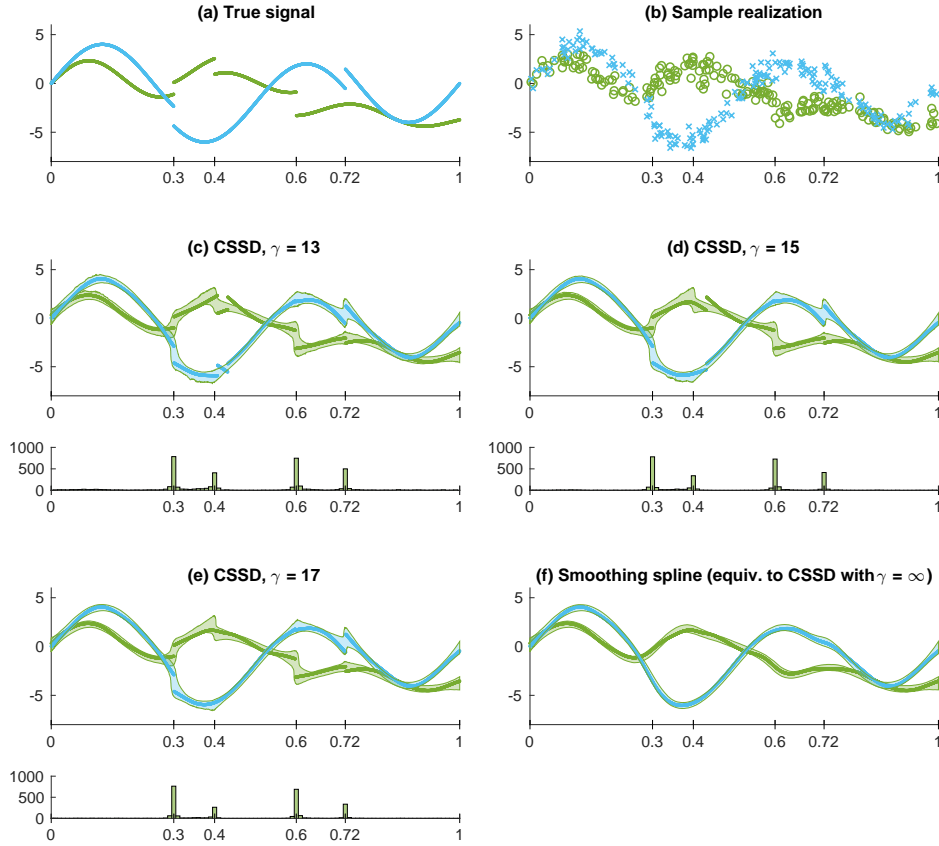


Figure 6: Here a y -value consists of two elements per data site x_i , so $y_i \in \mathbb{R}^2$: The first component are noisy samples of the signal used in Figure 1, rescaled by the factor 4, and the second component are noisy samples of the HeaviSine signal where $N = 200$, $\sigma = 0.6$. The description of the subplots matches that of Figure 1. Here $p = 0.9999$ was used.

A.3 Additional Experiments

A.3.1 Experiment on vector-valued data

Figure 6 shows a vector-valued variant of the last experiment. The data is generated according to $y_i = [4g_1(x_i), g_2(x_i)] + \epsilon_i \in \mathbb{R}^2$, for $i = 1, \dots, N$, where ϵ_i is a zero mean Gaussian random vector with $\sigma = 0.6$ in both components, and x consists of $N = 200$ random values uniformly distributed in the interval $[0, 1]$. The highest detection rate for discontinuities is observed at the shared discontinuity $x = 0.3$, and at the discontinuities $x = 0.6$ of g_1 and $x = 0.72$ of g_2 , which have a relatively large jump height. The discontinuity at $x = 0.4$ of g_1 has the lowest detection rate.

This is because jump height is relatively small and because the signal is smooth in the other component g_2 .

A.3.2 Detailed Runtimes for the Geyser data

The following table shows the runtimes for computing the CSSD solutions for the (p, γ) values sampled by the optimizer for determination of a hyperparameter using cross validation for the Geyser data. It illustrates the dependency of the runtime on the hyperparameters.

p	Parameters γ	Runtimes in seconds		
		Prop. + PELT	Prop. + FPVI	Baseline
0.590	526.700	0.367	0.173	60.084
0.114	527.176	0.012	0.010	59.848
0.646	0.429	0.085	0.066	1.419
0.493	0.658	0.077	0.069	1.510
0.103	527.187	0.011	0.010	59.577
0.513	4831.609	0.011	0.010	59.585
0.537	5312.121	0.011	0.010	59.474
0.614	7280.035	0.011	0.010	59.653
0.732	1.657	0.076	0.072	1.605
0.069	7280.580	0.011	0.010	59.745
0.144	0.044	0.074	0.062	1.362
0.114	7280.535	0.011	0.010	59.606
0.622	93608.646	0.011	0.010	60.009
0.947	0.155	0.074	0.061	1.320
0.653	7.335	0.076	0.097	2.088
0.273	0.212	0.075	0.064	1.441
0.331	93608.938	0.011	0.010	59.613
0.042	93609.227	0.011	0.010	59.796
0.387	93608.882	0.011	0.010	59.450
0.602	93608.666	0.011	0.010	59.565
0.651	4.694	0.076	0.086	1.871
0.002	93609.267	0.011	0.010	59.378
0.881	0.378	0.072	0.063	1.377
0.290	93608.979	0.011	0.010	59.654
0.631	0.681	0.073	0.065	1.488

0.236	93609.033	0.011	0.010	59.346
0.936	0.085	0.073	0.060	1.291
0.117	0.116	0.072	0.066	1.460
0.213	2.019	0.074	0.091	1.995
0.269	111546.763	0.012	0.011	59.621
0.124	111546.908	0.011	0.010	59.465
0.168	111546.863	0.011	0.010	59.401
0.111	111546.921	0.011	0.011	59.937
0.537	0.674	0.072	0.065	1.508
0.005	0.000	0.072	0.059	1.265
0.390	1.071	0.074	0.071	1.612
0.128	111546.903	0.011	0.010	59.407
0.098	0.325	0.074	0.072	1.673
0.444	0.782	0.073	0.068	1.554
0.107	111546.924	0.012	0.010	59.430
0.125	111546.907	0.011	0.010	59.994
0.029	0.008	0.072	0.062	1.350
0.888	6020996.048	0.011	0.010	59.499
0.936	11131354.260	0.011	0.010	59.545
0.756	6020996.178	0.011	0.011	59.938
0.962	49791138.958	0.011	0.010	60.057
0.990	0.383	0.073	0.063	1.377
0.120	0.017	0.073	0.062	1.311
0.971	64850739.923	0.011	0.010	59.546
0.978	1.358	0.075	0.067	1.537
0.983	114584785.015	0.011	0.010	59.512
0.070	0.066	0.073	0.064	1.483
0.604	1.018	0.072	0.067	1.564
0.307	49791139.591	0.011	0.010	59.506
0.870	749829891.245	0.011	0.010	59.635
0.213	0.069	0.072	0.062	1.353
0.080	749829916.274	0.011	0.010	59.557
0.270	1.039	0.074	0.074	1.707
0.014	749831228.153	0.011	0.010	59.465
0.305	0.941	0.072	0.072	1.668
0.073	0.715	0.075	0.095	2.003
0.065	749829704.341	0.012	0.011	59.438
0.021	0.007	0.074	0.063	1.354

0.024	749830030.862	0.011	0.011	59.601
0.767	0.260	0.071	0.061	1.352
0.043	749830566.931	0.011	0.010	59.629
0.004	0.000	0.073	0.062	1.286
0.268	3156327481.272	0.011	0.010	59.495
0.087	3156328930.084	0.011	0.011	59.785
0.005	0.001	0.073	0.065	1.340
0.069	0.258	0.074	0.074	1.692
0.047	3156329805.936	0.011	0.011	59.497
0.914	0.114	0.073	0.061	1.304
0.471	8.634	0.074	0.116	2.511
0.003	0.001	0.072	0.062	1.344
0.038	3156322261.285	0.011	0.011	59.484
0.018	3156324811.604	0.011	0.010	59.469
0.335	84810438426.386	0.011	0.010	59.853
0.607	259523504489.343	0.011	0.010	59.817
0.708	2.257	0.073	0.072	1.666
0.365	1.081	0.073	0.072	1.642
0.853	0.511	0.071	0.063	1.416
0.281	0.043	0.100	0.084	1.853
0.082	259535277319.531	0.011	0.011	60.145
0.610	5.918	0.074	0.092	2.011
0.079	592623241276.632	0.011	0.010	59.738
0.176	0.292	0.073	0.067	1.551
0.470	0.396	0.073	0.064	1.441
0.911	0.268	0.072	0.067	1.369
0.462	259528540565.781	0.011	0.010	59.687
0.039	0.009	0.071	0.062	1.338
0.949	0.136	0.073	0.062	1.305
0.162	259503123744.734	0.011	0.010	59.507
0.333	1.115	0.073	0.072	1.677
0.848	1.503	0.072	0.069	1.571
0.742	3938539941631.125	0.011	0.010	59.752
0.843	4.366	0.073	0.078	1.787
0.509	5364241589662.844	0.013	0.013	59.507
0.277	0.174	0.076	0.064	1.420
0.911	124337469315616.375	0.011	0.010	59.624
0.284	5365469498498.368	0.011	0.010	59.817

0.195	5.802	0.075	0.143	3.185
0.909	1.664	0.078	0.068	1.553
0.165	0.277	0.072	0.067	1.549
0.296	8127804155981.742	0.011	0.010	59.537
0.679	2.022	0.074	0.072	1.645
0.375	13670683942573.111	0.013	0.014	59.807
0.516	66360667692751.336	0.011	0.010	60.244
0.351	121661532746620.312	0.011	0.010	59.745
0.403	329737586174456.688	0.011	0.010	59.627
0.135	404951692953336.000	0.011	0.010	59.631
0.699	3.669	0.073	0.078	1.776
0.396	324434156222149.125	0.011	0.010	59.647
0.419	629523890588937.875	0.011	0.010	59.743
0.250	0.819	0.077	0.074	1.677
0.337	0.951	0.077	0.070	1.645
0.379	1707138347310834.500	0.012	0.010	59.658
0.479	2159475713125811.500	0.011	0.010	59.724
0.606	5459987574980714.000	0.011	0.010	59.548
0.612	5512629613117864.000	0.011	0.010	59.665
0.771	4.993	0.073	0.083	1.837
0.549	2.290	0.073	0.075	1.758
0.611	5506086000443386.000	0.011	0.010	59.356
0.621	Inf	0.029	0.025	0.071
0.788	17.290	0.076	0.131	2.767
0.591	Inf	0.007	0.007	0.069
0.591	Inf	0.008	0.007	0.069
0.499	3.784	0.074	0.087	1.887
0.514	Inf	0.008	0.007	0.070
0.610	Inf	0.007	0.007	0.069
0.708	13.420	0.075	0.118	2.552
0.489	7.056	0.074	0.107	2.258
0.671	7.459	0.074	0.096	2.064
0.531	5.308	0.074	0.094	2.027
0.632	6.025	0.073	0.091	2.007
0.688	44.021	0.084	0.196	5.208
0.527	7.254	0.075	0.105	2.219
0.520	9.342	0.074	0.115	2.475
0.636	8.280	0.074	0.102	2.155

0.634	Inf	0.007	0.007	0.069
0.647	Inf	0.008	0.007	0.069
0.647	8.298	0.075	0.101	2.163
0.641	Inf	0.007	0.007	0.069
0.681	12.506	0.075	0.117	2.511
0.597	Inf	0.007	0.007	0.069
0.586	9.545	0.074	0.110	2.343
0.580	10.332	0.075	0.118	2.448
0.626	Inf	0.007	0.007	0.069
0.638	21.280	0.076	0.151	3.344
0.626	15.701	0.075	0.133	2.937
0.597	12.514	0.075	0.123	2.663
0.619	16.092	0.075	0.136	2.970
0.590	Inf	0.007	0.007	0.069
0.558	Inf	0.008	0.007	0.069
0.565	Inf	0.007	0.007	0.069
0.600	177.147	0.310	0.237	55.215
0.582	19.708	0.075	0.150	3.349
0.571	Inf	0.007	0.007	0.070
0.548	Inf	0.008	0.007	0.072
0.571	Inf	0.007	0.007	0.069
0.574	Inf	0.007	0.007	0.070
0.579	Inf	0.007	0.007	0.070
0.570	24.386	0.078	0.165	3.846
0.588	26.507	0.079	0.168	3.948
0.601	316.812	0.356	0.201	59.377
0.590	Inf	0.008	0.007	0.070
0.586	Inf	0.007	0.007	0.070
0.586	Inf	0.007	0.007	0.069
0.592	Inf	0.008	0.007	0.070
0.582	Inf	0.008	0.007	0.072
0.584	Inf	0.008	0.007	0.071
0.570	85.987	0.153	0.237	21.792
0.598	141.375	0.265	0.248	45.122
0.579	Inf	0.007	0.007	0.069
0.575	Inf	0.007	0.007	0.071
0.563	100.374	0.188	0.244	28.257
0.581	Inf	0.007	0.007	0.069

0.579	Inf	0.007	0.007	0.069
0.589	92.531	0.159	0.239	23.093
0.570	1388.299	0.324	0.057	59.622
0.580	191.365	0.341	0.232	59.389
0.572	1901.378	0.331	0.021	59.657
0.574	65.244	0.113	0.238	12.072
0.577	83.798	0.149	0.236	20.770
0.570	2526.015	0.011	0.010	59.525
0.567	4962.193	0.011	0.010	59.506
0.568	6062.057	0.011	0.010	59.474
0.572	85.528	0.153	0.239	21.311
0.568	87.614	0.157	0.240	22.452
0.568	5327.694	0.011	0.010	59.446
0.567	19544.473	0.012	0.010	59.602
0.574	14277.543	0.012	0.010	59.736
0.571	41111.586	0.012	0.011	59.361
0.571	45632.944	0.011	0.010	59.523
0.575	319.334	0.325	0.197	59.598
0.571	159.842	0.299	0.237	52.875
0.574	1320.864	0.325	0.065	59.563
0.571	320.369	0.324	0.194	60.013
0.579	255.318	0.325	0.214	59.425
0.583	598.731	0.327	0.154	59.590
0.580	198.514	0.323	0.229	59.197
0.582	970.506	0.323	0.113	59.618
0.585	281.439	0.326	0.209	59.581
0.585	317.095	0.331	0.199	59.665
0.588	436.217	0.326	0.195	59.622
0.588	806.310	0.327	0.129	59.383
0.588	1771.145	0.325	0.026	59.596
0.587	154.362	0.290	0.239	50.747
0.587	162.405	0.300	0.239	52.917
0.587	701.035	0.326	0.142	59.551
0.586	202.210	0.324	0.229	59.416
0.585	166.308	0.302	0.237	53.425
0.586	122.144	0.227	0.249	36.514
0.588	244.594	0.324	0.216	59.540
0.590	209.887	0.324	0.229	59.549

0.588	149.229	0.280	0.240	50.307
0.588	683.330	0.324	0.144	59.557
0.587	527.589	0.327	0.166	59.472
0.587	235.829	0.325	0.218	59.513
0.586	214.067	0.357	0.251	59.867
0.586	146.380	0.290	0.263	48.902
0.586	380.009	0.327	0.193	59.442
0.586	151.147	0.285	0.240	49.792
0.585	338.013	0.326	0.194	59.562
0.585	212.139	0.327	0.227	59.551
0.585	221.865	0.343	0.222	59.680
0.584	324.003	0.324	0.196	59.417
0.584	424.976	0.325	0.186	59.551
0.585	240.241	0.326	0.218	59.518
0.584	288.379	0.325	0.208	59.566
0.583	278.994	0.359	0.211	59.545
0.584	236.488	0.323	0.217	59.655
0.584	204.407	0.328	0.229	59.292
0.585	200.578	0.326	0.231	59.411
0.585	252.444	0.326	0.213	59.361
0.584	226.093	0.325	0.220	59.586
0.584	219.866	0.327	0.223	59.821
0.583	189.203	0.322	0.231	58.748
0.584	269.579	0.328	0.213	59.501
0.584	246.401	0.324	0.214	59.445
0.584	300.942	0.324	0.205	59.570
0.585	259.173	0.329	0.240	59.492
0.585	231.096	0.326	0.219	59.448
0.585	220.403	0.325	0.222	59.357
0.585	206.871	0.324	0.228	59.540
0.585	205.195	0.346	0.234	59.375
0.585	187.338	0.323	0.233	58.824
0.585	232.905	0.324	0.218	59.724
0.585	213.151	0.325	0.226	59.552
0.585	256.912	0.326	0.212	59.425
0.585	263.081	0.327	0.212	59.478
0.585	274.135	0.327	0.213	59.455
0.585	240.549	0.328	0.217	59.787

0.585	219.840	0.324	0.223	59.714
0.585	220.320	0.327	0.224	59.531
0.585	220.357	0.327	0.223	59.561
0.585	228.991	0.327	0.222	59.578
0.801	0.732	0.072	0.064	1.469
0.411	220.493	0.326	0.205	59.531
0.368	3.030	0.074	0.089	1.938
0.878	2268.890	0.329	0.036	60.102
0.218	0.245	0.073	0.065	1.498
0.504	320.227	0.327	0.194	59.789
0.316	320.415	0.324	0.156	59.705
0.805	2866.386	0.137	0.014	59.776
0.475	0.686	0.072	0.066	1.526
0.397	0.386	0.072	0.064	1.481
0.986	0.077	0.073	0.061	1.286
0.936	10219.400	0.011	0.010	59.584
0.940	0.420	0.072	0.063	1.379
0.733	2866.458	0.011	0.010	59.725
0.776	3623.137	0.011	0.010	59.580
0.986	0.063	0.072	0.060	1.276
0.972	0.142	0.072	0.062	1.313
0.936	0.375	0.073	0.063	1.367
0.775	491.181	0.326	0.196	59.963
0.760	35.515	0.081	0.172	4.021
0.792	9.722	0.075	0.100	2.147
0.842	757.211	0.363	0.210	59.746
0.757	6.737	0.075	0.091	1.958
0.826	41.892	0.082	0.177	4.256
0.954	0.389	0.077	0.062	1.392
0.725	757.328	0.324	0.152	59.450
0.964	0.146	0.072	0.061	1.302
0.358	757.694	0.325	0.091	59.511
0.788	1068.939	0.376	0.129	59.526
0.016	758.036	0.011	0.010	59.686
0.497	0.520	0.072	0.066	1.490
0.635	0.120	0.071	0.061	1.321
0.500	0.516	0.072	0.067	1.487
0.005	0.002	0.074	0.063	1.372

0.758	141752.089	0.011	0.010	59.859
0.021	141752.827	0.011	0.010	59.758
0.906	0.575	0.077	0.064	1.418
0.189	141752.658	0.011	0.010	59.735
0.192	50.076	0.249	0.235	43.479
0.233	184568.319	0.011	0.010	60.853
0.193	0.933	0.074	0.077	1.765
0.204	184568.348	0.011	0.010	59.845
0.812	0.251	0.072	0.062	1.366
0.177	184568.376	0.011	0.010	59.615
0.377	4.032	0.075	0.097	2.054
0.624	1426630.338	0.011	0.010	59.816
0.013	1426630.953	0.013	0.011	60.181
1.000	2860787717.945	0.011	0.010	59.780
0.529	1426630.433	0.011	0.010	59.866
0.345	1426630.617	0.011	0.010	59.951
0.393	1749706.701	0.011	0.010	59.827
0.055	0.009	0.072	0.061	1.320
0.322	1749706.772	0.011	0.010	60.040
0.528	1.850	0.073	0.073	1.686
0.580	3737916.743	0.011	0.010	59.587
0.687	0.885	0.073	0.066	1.502
0.114	3737917.202	0.011	0.010	59.558
0.035	0.002	0.073	0.060	1.285
0.798	0.742	0.074	0.065	1.471
0.367	0.628	0.072	0.067	1.558
0.111	0.026	0.073	0.062	1.332
0.618	4850129.417	0.011	0.010	59.596
0.070	4850129.964	0.011	0.010	59.880
0.200	4850129.835	0.013	0.010	59.901
0.444	17668726.997	0.011	0.010	59.677
0.012	17668726.773	0.019	0.014	59.740
0.976	903411595.871	0.011	0.010	59.739
0.336	1.053	0.074	0.072	1.661
0.021	17668727.717	0.013	0.012	59.654
0.194	17668727.309	0.012	0.010	59.944
0.116	0.002	0.072	0.059	1.278
0.617	194792242.976	0.011	0.010	59.613

0.537	194792242.983	0.011	0.010	59.758
0.667	246512874.385	0.011	0.011	59.689
0.784	0.374	0.072	0.064	1.385
0.136	0.069	0.072	0.063	1.385
0.693	277821994.112	0.011	0.010	59.817
0.985	0.352	0.074	0.064	1.376
0.974	4560942816.065	0.011	0.010	59.713
0.961	2.948	0.073	0.072	1.658
0.918	1.690	0.073	0.070	1.562
0.330	667273213.769	0.011	0.010	59.754
0.824	2.849	0.073	0.073	1.689
0.667	558165477.439	0.011	0.010	59.890
0.356	1138187199.732	0.011	0.010	59.687
0.481	3152915556.843	0.011	0.010	59.963
0.145	0.137	0.074	0.065	1.462
0.063	0.095	0.074	0.066	1.539
0.903	1.672	0.073	0.068	1.572
0.520	0.458	0.073	0.065	1.450
0.398	6970431007.219	0.011	0.012	59.865
0.664	0.838	0.073	0.069	1.519
0.290	18593622892.776	0.011	0.010	59.690
0.683	1.113	0.073	0.067	1.548
0.209	0.487	0.073	0.069	1.610
0.782	2.523	0.072	0.071	1.679
0.809	4.573	0.072	0.080	1.821
0.819	18.020	0.075	0.125	2.761
0.446	3961319101.063	0.011	0.010	59.557
0.646	1.754	0.072	0.070	1.618
0.529	6021413455.407	0.011	0.010	59.665
0.643	1.806	0.073	0.070	1.643
0.573	8078511273.050	0.011	0.011	59.902
0.512	11200655447.203	0.011	0.011	59.809
0.410	27028796962.588	0.011	0.010	60.192
0.413	1.545	0.073	0.073	1.694
0.644	3.023	0.074	0.078	1.760
0.606	28013601706.505	0.011	0.010	59.635
0.722	215766869821.222	0.011	0.010	59.834
0.597	2.529	0.073	0.076	1.735

0.617	39167051592.785	0.011	0.010	59.691
0.761	11.652	0.075	0.109	2.318
0.498	3.660	0.073	0.086	1.884
0.619	70901713895.259	0.011	0.010	59.897
0.649	102979116175.764	0.011	0.010	59.926
0.492	9.724	0.075	0.120	2.581
0.512	6.502	0.075	0.102	2.136
0.649	4.635	0.073	0.086	1.884
0.589	97634640654.249	0.011	0.010	60.167
0.594	129082124643.546	0.011	0.010	59.889
0.515	6.780	0.075	0.103	2.192
0.495	65.722	0.132	0.232	17.448
0.616	5.843	0.074	0.092	2.006
0.518	799767184544.176	0.011	0.010	59.930
0.626	7.004	0.075	0.097	2.084
0.625	511759365087.038	0.011	0.010	59.898
0.687	13.999	0.075	0.121	2.622
0.686	4427757963162.376	0.011	0.010	59.772
0.693	73.280	0.107	0.228	10.459
0.689	42.197	0.083	0.187	4.989
0.664	7159009816912.056	0.011	0.010	60.008
0.684	12816707988126.680	0.011	0.010	59.987
0.654	10.646	0.074	0.112	2.378
0.661	8452732907111.057	0.011	0.010	59.648
0.675	15990489622285.115	0.011	0.010	59.699
0.684	25571390347055.973	0.011	0.010	59.752
0.691	14.713	0.076	0.124	2.722
0.679	18748202365346.027	0.011	0.010	59.764
0.646	19.848	0.075	0.145	3.223
0.674	20991466988591.750	0.011	0.010	59.758
0.674	24181896617711.914	0.011	0.010	59.673
0.701	191212223070708.406	0.011	0.010	59.973
0.721	24.808	0.075	0.151	3.394
0.681	1226545502631163.000	0.011	0.010	59.661
0.691	2073180576847488.750	0.011	0.010	59.791
0.718	86.758	0.119	0.232	14.056
0.708	31.191	0.079	0.168	3.875
0.701	Inf	0.007	0.007	0.070

0.693	2081895416906701.750	0.011	0.010	59.635
0.683	28.537	0.079	0.167	3.778
0.713	154.971	0.269	0.276	41.226
0.692	30.643	0.079	0.167	3.919
0.685	3086538429085923.500	0.011	0.010	59.588
0.692	36.496	0.081	0.178	4.402
0.693	38.983	0.083	0.183	4.663
0.690	6219242342265599.000	0.011	0.010	59.625
0.695	47.999	0.085	0.198	5.637
0.677	48.044	0.086	0.198	5.851
0.694	55.528	0.089	0.206	6.787
0.673	90.304	0.135	0.233	18.002
0.698	122.312	0.187	0.248	28.449
0.674	112.177	0.173	0.248	26.154
0.682	Inf	0.007	0.007	0.070
0.679	Inf	0.007	0.007	0.070
0.678	59.382	0.095	0.213	7.774
0.679	Inf	0.007	0.007	0.070
0.687	Inf	0.007	0.007	0.070
0.680	Inf	0.008	0.007	0.072
0.671	Inf	0.007	0.007	0.070
0.671	Inf	0.007	0.007	0.071
0.673	Inf	0.007	0.007	0.070
0.676	101.669	0.153	0.241	21.818
0.675	107.423	0.164	0.246	24.095
0.666	157.310	0.277	0.242	46.048
0.670	Inf	0.007	0.007	0.070
0.664	Inf	0.008	0.007	0.071
0.668	133.222	0.219	0.250	34.511
0.669	379.312	0.325	0.195	59.659
0.665	123.180	0.209	0.248	30.642
0.668	171.878	0.288	0.239	50.540
0.665	Inf	0.007	0.007	0.071
0.669	Inf	0.007	0.007	0.071
0.672	222.089	0.332	0.232	59.478
0.666	Inf	0.007	0.007	0.070
0.666	Inf	0.007	0.007	0.070
0.663	234.973	0.325	0.230	59.647

0.660	1083.052	0.327	0.114	60.114
0.661	160.226	0.274	0.243	48.177
0.659	194.596	0.315	0.242	56.736
0.660	47664.792	0.011	0.010	59.878
0.660	55898.733	0.011	0.010	59.674
0.663	1015375.549	0.011	0.010	59.802
0.662	388682.629	0.011	0.010	59.669
0.662	292.559	0.338	0.218	59.421
0.662	980.899	0.325	0.123	59.456
0.664	224.976	0.325	0.232	59.425
0.665	140.490	0.227	0.244	37.439
0.664	132.812	0.218	0.249	34.695
0.665	507.969	0.325	0.181	59.527
0.665	179.657	0.300	0.243	52.979
0.665	416.509	0.369	0.208	59.531
0.664	142.186	0.235	0.246	39.006
0.663	156.999	0.265	0.244	46.244
0.664	466.869	0.328	0.190	59.875
0.663	235.292	0.326	0.230	59.736
0.663	464.810	0.327	0.188	59.625
0.664	327.750	0.340	0.235	59.651
0.662	447.701	0.325	0.192	59.571
0.661	337.118	0.323	0.204	59.729
0.662	305.454	0.325	0.212	59.659
0.662	237.961	0.332	0.227	59.733
0.660	612.928	0.326	0.161	59.886
0.661	482.168	0.326	0.185	59.888
0.661	288.823	0.345	0.212	59.830
0.662	419.973	0.325	0.193	59.929
0.662	231.846	0.326	0.230	59.835
0.660	299.707	0.324	0.213	59.693
0.661	352.747	0.328	0.203	59.857
0.661	359.407	0.326	0.197	59.554
0.661	252.961	0.326	0.223	59.683
0.661	393.824	0.326	0.195	59.763
0.661	620.260	0.351	0.175	59.531
0.661	408.419	0.350	0.208	59.654
0.661	468.257	0.328	0.188	59.576

0.661	317.841	0.328	0.211	59.755
0.660	381.932	0.367	0.196	59.881
0.660	359.344	0.325	0.197	59.636
0.660	452.253	0.345	0.192	59.565
0.659	421.150	0.341	0.195	59.663
0.659	534.327	0.330	0.177	59.561
0.659	413.488	0.327	0.194	59.599
0.659	405.629	0.324	0.194	59.823
0.658	339.945	0.327	0.203	59.686
0.658	291.639	0.327	0.213	59.525
0.658	257.297	0.326	0.220	59.538
0.659	274.706	0.328	0.217	59.547
0.658	263.283	0.330	0.219	61.696
0.658	246.145	0.329	0.224	59.640
0.658	274.522	0.341	0.217	59.711
0.658	290.296	0.325	0.213	59.702
0.658	257.259	0.351	0.231	59.481
0.658	265.088	0.327	0.238	59.603
0.658	238.496	0.343	0.226	59.880
0.658	248.352	0.335	0.223	59.640
0.658	270.627	0.330	0.228	59.634
0.657	259.843	0.327	0.219	59.534
0.657	265.855	0.328	0.220	59.650
0.657	265.286	0.328	0.218	59.616
0.657	252.862	0.330	0.220	59.807
0.657	266.438	0.356	0.220	59.763
0.657	262.683	0.334	0.220	59.721
0.657	277.166	0.329	0.216	59.825
0.657	271.137	0.326	0.217	59.814
0.657	261.274	0.325	0.219	60.159
0.657	283.040	0.326	0.213	59.976
0.657	274.177	0.332	0.215	59.670
0.657	285.901	0.325	0.213	59.564
0.657	281.740	0.326	0.214	59.535
0.657	281.783	0.328	0.218	59.807
0.657	294.420	0.334	0.214	59.772
0.939	0.202	0.073	0.061	1.331
0.702	4.544	0.073	0.083	1.849

0.242	282.155	0.327	0.147	59.742
0.374	0.490	0.072	0.065	1.520
0.760	466.612	0.326	0.195	59.979
0.134	467.238	0.332	0.023	59.827
0.685	6545.861	0.011	0.010	59.656
0.565	6545.981	0.011	0.010	59.496
0.756	1.165	0.074	0.068	1.546
0.335	0.486	0.074	0.067	1.528
0.705	1.486	0.076	0.071	1.605
0.873	0.361	0.073	0.063	1.390
0.156	0.060	0.072	0.062	1.388
0.002	0.000	0.073	0.059	1.252
0.410	1.234	0.074	0.075	1.637
0.103	6546.443	0.011	0.010	59.638
0.331	0.970	0.074	0.071	1.639
0.265	17.715	0.084	0.189	5.383
0.143	9500.861	0.011	0.010	59.549
0.078	9500.926	0.011	0.010	59.670
0.044	0.457	0.074	0.095	2.044
0.800	448435.274	0.011	0.010	60.044
0.539	1.110	0.074	0.069	1.592
0.734	448435.340	0.011	0.010	59.603
0.616	3.230	0.074	0.080	1.780
0.516	448435.559	0.011	0.010	59.606
0.905	4033274.169	0.011	0.010	59.627
0.666	1.482	0.074	0.070	1.609
0.619	685369.307	0.011	0.010	59.860
0.016	685369.910	0.011	0.010	59.705
0.107	0.684	0.073	0.083	1.837
0.262	685369.664	0.011	0.010	59.641
0.435	882889.526	0.011	0.011	59.900
0.111	0.024	0.073	0.062	1.340
0.364	0.518	0.073	0.067	1.543
0.842	0.967	0.073	0.066	1.509
0.084	685369.842	0.011	0.010	60.074
0.603	1.340	0.073	0.071	1.619
0.436	1.040	0.072	0.069	1.619
0.357	0.713	0.072	0.069	1.597

0.596	30.318	0.080	0.175	4.249
0.647	11.281	0.076	0.116	2.456
0.627	709560.291	0.012	0.010	59.543
0.989	0.216	0.074	0.063	1.346
0.969	0.226	0.073	0.062	1.347
0.829	2044292.561	0.011	0.010	59.607
0.316	2044293.076	0.011	0.010	59.988
0.147	2044293.245	0.011	0.010	59.890
0.144	24.249	0.169	0.234	25.167
0.243	3827638.346	0.011	0.010	60.035
0.291	1055.237	0.263	0.019	59.976
0.510	11.551	0.076	0.135	2.805
0.254	3.922	0.074	0.110	2.318
0.191	1055.336	0.011	0.011	59.542
0.217	3.558	0.078	0.115	2.365
0.804	10564.758	0.011	0.010	59.759
0.975	100912.115	0.012	0.010	59.669
0.511	10565.051	0.011	0.010	59.686
0.085	10565.478	0.011	0.010	59.727
0.349	0.581	0.074	0.068	1.562
0.725	26642.267	0.011	0.010	60.042
0.956	2.715	0.073	0.070	1.639
0.216	3.096	0.075	0.107	2.276
0.797	39832.931	0.011	0.010	59.731
0.176	26642.816	0.011	0.010	59.738
0.288	50585.543	0.011	0.010	59.957
0.283	76169.176	0.011	0.010	59.903
0.255	76169.205	0.011	0.010	59.826
0.545	7.381	0.074	0.104	2.180
0.056	76169.404	0.011	0.012	61.370
0.257	472.236	0.327	0.111	59.877
0.225	472.269	0.328	0.095	59.626
0.913	14331.158	0.011	0.010	59.906
0.955	29260.486	0.011	0.010	59.694
0.033	0.279	0.073	0.089	1.964
0.956	11.869	0.075	0.101	2.152
0.623	23821.607	0.011	0.010	59.859
0.608	1705.329	0.326	0.034	60.340

0.504	1705.434	0.328	0.021	60.015
0.372	1938.379	0.013	0.011	59.900
0.923	39082.740	0.011	0.010	59.771
0.958	115916.689	0.012	0.010	60.073
0.678	5.539	0.079	0.093	1.916
0.906	52806.719	0.011	0.011	59.998
0.469	5.523	0.078	0.102	2.117
0.936	80738.218	0.011	0.010	60.092
0.387	10.228	0.075	0.136	2.977
0.988	24.674	0.074	0.136	2.951
0.935	80859.645	0.011	0.010	59.921
0.590	9.317	0.074	0.110	2.355
0.951	108856.803	0.011	0.010	59.729
0.826	10.836	0.074	0.102	2.188
0.948	12.746	0.076	0.104	2.189
0.950	105873.198	0.011	0.010	59.959
0.792	177115.194	0.011	0.010	60.006
0.987	33.039	0.075	0.155	3.374
0.455	24.626	0.081	0.179	4.517
0.831	228642.599	0.011	0.010	59.912
0.948	20.327	0.076	0.125	2.733
0.895	238.351	0.311	0.235	55.140
0.928	1226.927	0.324	0.128	59.750
0.780	182799.131	0.011	0.010	59.788
0.785	18.143	0.075	0.129	2.829
0.998	21849199.618	0.012	0.011	59.826
0.677	289776.619	0.011	0.010	59.987
0.681	395189.276	0.011	0.010	60.088
0.641	472210.561	0.011	0.010	59.904
0.805	6695909.183	0.011	0.010	59.990
0.824	13303668.818	0.011	0.010	59.902
0.777	26.387	0.076	0.152	3.367
0.835	29.973	0.075	0.156	3.428
0.878	36.501	0.079	0.167	3.767
0.696	35641614.296	0.011	0.010	59.811
0.825	67.667	0.090	0.210	6.987
0.806	56.180	0.087	0.199	5.679
0.616	114358639.537	0.011	0.011	59.767

0.642	167063374.456	0.011	0.010	60.002
0.568	406776777.747	0.011	0.010	59.846
0.562	787632447.603	0.011	0.010	59.917
0.577	1706494891.781	0.011	0.010	59.924
0.553	2145958427.359	0.011	0.010	59.953
0.454	1913.307	0.011	0.011	59.832
0.612	52.660	0.093	0.211	7.643
0.604	51.450	0.100	0.220	7.544
0.609	59.745	0.101	0.228	9.061
0.516	5493512304.546	0.011	0.010	59.659
0.534	3107399906.930	0.011	0.010	59.683
0.574	3303242016.801	0.011	0.011	60.002
0.525	11776545164.624	0.011	0.010	59.782
0.574	3460165353.872	0.012	0.011	59.669
0.567	3952652174.790	0.011	0.010	60.038
0.512	143.477	0.298	0.239	52.297
0.567	3977018854.510	0.011	0.010	59.819
0.599	86.492	0.149	0.238	20.941
0.575	71.697	0.125	0.241	15.312
0.603	115.996	0.217	0.289	32.761
0.579	38607239762.448	0.011	0.010	59.796
0.537	314.634	0.325	0.194	59.771
0.556	102.439	0.195	0.246	30.083
0.618	821.897	0.327	0.134	59.919
0.589	52273131624.919	0.011	0.010	59.745
0.601	113.246	0.207	0.250	31.546
0.622	524.960	0.325	0.171	59.878
0.630	918.233	0.326	0.124	59.742
0.645	2916.934	0.011	0.010	59.920
0.617	643.895	0.326	0.153	59.860
0.606	1575.093	0.326	0.041	59.649
0.598	2330.248	0.011	0.010	59.696
0.596	2608.364	0.011	0.010	59.661
0.612	9316.068	0.011	0.010	59.772
0.625	211.484	0.324	0.231	59.768
0.639	1516.464	0.329	0.058	59.721
0.608	129.517	0.273	0.272	40.271
0.638	815.469	0.325	0.136	59.727

0.628	5546.180	0.011	0.010	59.914
0.646	118845.773	0.011	0.010	59.802
0.643	215390.153	0.011	0.010	59.970
0.613	1296.515	0.326	0.080	59.875
0.622	3752.972	0.011	0.010	59.969
0.620	261.580	0.330	0.218	60.024
0.607	210.972	0.325	0.231	60.094
0.613	536.069	0.325	0.183	60.376
0.610	594.334	0.324	0.157	59.938
0.607	1452.214	0.325	0.059	59.953
0.604	288.037	0.378	0.212	60.259
0.612	187.427	0.317	0.237	57.590
0.614	325.823	0.326	0.252	59.694
0.612	444.801	0.326	0.186	59.799
0.605	1036.036	0.326	0.110	59.949
0.608	3350.272	0.011	0.010	59.835
0.606	434.444	0.325	0.187	59.698
0.611	273.998	0.327	0.214	59.799
0.599	500.917	0.325	0.174	60.101
0.592	455.498	0.326	0.182	59.817
0.588	276.833	0.323	0.212	59.739
0.594	259.408	0.327	0.215	59.782
0.599	220.198	0.325	0.226	59.762
0.596	402.612	0.328	0.194	59.842
0.596	389.534	0.338	0.207	60.030
0.591	198.440	0.328	0.232	59.780
0.593	384.081	0.326	0.194	59.800
0.592	717.207	0.327	0.141	60.277
0.588	1067.466	0.326	0.107	59.788
0.587	5894.724	0.011	0.010	59.857
0.585	222291.257	0.011	0.010	59.957
0.589	8216.089	0.011	0.010	59.890
0.586	1060.109	0.326	0.106	59.876
0.589	1742.865	0.324	0.028	59.869
0.585	6483.139	0.011	0.010	59.886
0.585	8697.775	0.011	0.010	60.391
0.584	1084.219	0.324	0.104	59.838
0.586	707.404	0.328	0.141	59.896

0.588	554.726	0.327	0.161	60.067
0.586	1298.514	0.325	0.069	60.017
0.586	722.931	0.336	0.139	59.819
0.584	999.145	0.324	0.110	60.081
0.588	1393.049	0.324	0.059	59.891
0.586	946.429	0.326	0.116	59.824
0.588	867.984	0.327	0.123	60.127
0.589	1454.795	0.323	0.053	60.071
0.589	670.400	0.326	0.146	60.060
0.590	520.218	0.328	0.169	59.971
0.591	620.154	0.326	0.173	60.833
0.589	453.912	0.328	0.182	60.061
0.589	547.750	0.340	0.163	59.853
0.590	586.536	0.334	0.155	60.027
0.590	490.535	0.348	0.174	60.185
0.591	498.826	0.326	0.179	60.074
0.591	441.626	0.325	0.185	59.806
0.590	414.726	0.324	0.190	59.752
0.590	465.110	0.326	0.179	59.886
0.589	476.858	0.323	0.176	60.116
0.589	428.230	0.346	0.198	60.969
0.589	465.458	0.325	0.180	59.957
0.589	465.536	0.326	0.181	59.892
0.589	505.474	0.324	0.171	59.804
0.055	0.006	0.072	0.060	1.309
0.993	47117.747	0.011	0.010	60.115
0.151	0.052	0.072	0.062	1.368
0.685	704.607	0.324	0.153	59.758
0.197	465.850	0.324	0.073	59.882
0.301	0.314	0.072	0.064	1.486
0.019	0.001	0.074	0.061	1.268
0.845	1775.606	0.326	0.069	59.974
0.905	3081.594	0.198	0.015	59.726
0.322	3082.177	0.011	0.010	59.995
0.749	19431.898	0.011	0.010	59.877
0.374	19432.273	0.011	0.010	59.842
0.777	6.172	0.074	0.088	1.917
0.651	19431.996	0.011	0.010	59.819

0.794	40280.291	0.011	0.010	60.006
0.499	1.638	0.073	0.072	1.699
0.918	117506.746	0.011	0.010	59.704
0.992	0.113	0.072	0.061	1.307
0.949	192559.783	0.011	0.010	59.981
0.959	0.953	0.073	0.065	1.489
0.991	0.120	0.073	0.061	1.311
0.995	0.072	0.072	0.061	1.283
0.955	0.237	0.073	0.062	1.341
0.957	233353.240	0.011	0.010	59.975
0.978	469444.897	0.011	0.010	60.179
0.346	0.195	0.073	0.064	1.409
0.988	827200.215	0.011	0.010	59.852
0.982	585131.330	0.011	0.010	59.909
0.746	12.210	0.074	0.111	2.370
0.991	0.975	0.073	0.064	1.483
0.986	742415.091	0.012	0.012	60.218
0.116	0.016	0.072	0.060	1.310
0.983	595647.232	0.011	0.010	59.953
0.985	690502.152	0.011	0.010	59.899
0.988	6.150	0.074	0.083	1.840
0.343	690502.795	0.011	0.010	60.031
0.032	0.022	0.074	0.064	1.439
0.281	1130573.652	0.011	0.010	59.877
0.465	1152377.623	0.011	0.010	59.633
0.008	1152378.075	0.011	0.010	59.835
0.470	103.182	0.237	0.243	39.585
0.078	0.115	0.075	0.068	1.525
0.273	0.875	0.073	0.072	1.670
0.996	0.253	0.073	0.065	1.341
0.314	0.764	0.076	0.070	1.606
0.702	3115633.835	0.011	0.010	59.927
0.709	197.165	0.327	0.251	55.115
0.918	1.053	0.073	0.065	1.506
0.756	11.501	0.077	0.109	2.299
0.985	1.169	0.074	0.066	1.497
0.224	3115634.314	0.013	0.011	59.924
0.061	3115634.484	0.011	0.011	59.894

0.577	1.739	0.072	0.071	1.659
0.014	3115634.538	0.011	0.010	59.839
0.005	3115634.649	0.011	0.010	59.683
0.872	1545285041.534	0.011	0.010	59.730
0.960	5393692074.840	0.011	0.010	59.860
0.741	6332203425.481	0.011	0.010	60.122
0.245	0.666	0.073	0.071	1.628
0.700	34005997393.719	0.011	0.010	59.697
0.925	178508442385.008	0.011	0.011	59.772
0.791	1.178	0.073	0.066	1.522
0.167	0.457	0.073	0.073	1.637
0.590	1.055	0.072	0.068	1.576
0.695	1.333	0.072	0.068	1.589
0.963	383597419354.126	0.011	0.012	60.151
0.652	9.898	0.074	0.116	2.302
0.333	0.871	0.074	0.071	1.625
0.284	383623467629.082	0.011	0.010	60.077
0.042	0.304	0.074	0.089	1.899
0.688	23.057	0.077	0.152	3.374
0.887	7617592179610.292	0.011	0.010	60.007
0.191	2.610	0.074	0.104	2.215
0.018	0.099	0.076	0.079	1.798
0.633	7.423	0.079	0.100	2.133
0.237	386274706452.496	0.012	0.010	59.991
0.084	0.684	0.075	0.089	1.924
0.171	386312491677.862	0.011	0.010	59.784
0.151	27.990	0.186	0.238	28.046
0.517	2.956	0.072	0.079	1.821
0.185	1.032	0.074	0.081	1.819
0.191	2981911061482.812	0.011	0.010	59.986
0.280	6245404225656.586	0.011	0.010	59.844
0.841	8.458	0.074	0.094	2.031
0.139	6245997128421.129	0.011	0.010	59.716
0.162	21.193	0.147	0.223	17.020
0.881	17.196	0.075	0.130	2.557
0.205	6245105393704.646	0.011	0.010	59.945
0.253	8412959803646.695	0.011	0.011	59.814
0.220	24.882	0.111	0.219	11.942

0.794	73.066	0.099	0.221	8.399
0.201	10923566517951.732	0.013	0.012	59.846
0.244	8547530231286.136	0.013	0.011	59.857
0.672	20.993	0.083	0.146	3.235
0.109	9951417967484.533	0.011	0.010	59.756
0.624	19.951	0.076	0.149	3.245
0.411	6.351	0.075	0.111	2.350
0.382	22370338012261.215	0.011	0.010	59.982
0.720	32.881	0.079	0.170	3.988
0.519	56274212548869.945	0.011	0.010	59.828
0.656	144192921258535.781	0.012	0.012	59.880
0.437	8.327	0.074	0.119	2.553
0.541	91975695336001.891	0.011	0.010	60.017
0.512	143983221610210.219	0.011	0.010	59.875
0.548	102855963667673.109	0.011	0.010	61.172
0.371	238487650265725.344	0.011	0.010	60.280
0.186	559893279455930.562	0.012	0.010	59.998
0.205	462245679643149.188	0.011	0.010	60.016
0.159	Inf	0.007	0.007	0.072
0.367	330588552745522.938	0.011	0.010	59.972
0.555	64.393	0.132	0.230	12.684
0.260	2340894367898804.000	0.012	0.011	59.872
0.436	3492.062	0.011	0.010	59.854
0.573	34.754	0.082	0.186	4.915
0.510	24618.782	0.011	0.010	60.117
0.600	71748.845	0.011	0.010	59.896
0.467	49.560	0.109	0.223	10.525
0.577	90766.870	0.012	0.011	59.755
0.589	102844.673	0.011	0.011	59.719
0.558	239987.409	0.011	0.010	60.224
0.624	166084.237	0.011	0.010	59.738
0.574	320092.383	0.011	0.010	59.905
0.649	51.653	0.089	0.205	6.731
0.474	12366.182	0.011	0.010	60.046
0.638	2229507.924	0.011	0.010	59.843
0.513	1030632.652	0.011	0.010	59.826
0.517	1208088.440	0.011	0.010	59.781
0.575	6306875.043	0.011	0.010	59.893

0.639	84.843	0.133	0.233	17.698
0.539	50.098	0.098	0.219	8.564
0.592	14643905.161	0.012	0.011	59.949
0.535	92.901	0.180	0.244	27.068
0.649	137.113	0.229	0.248	37.674
0.619	83306376.307	0.011	0.010	59.772
0.568	65.275	0.113	0.231	12.502
0.646	7590.711	0.011	0.010	59.949
0.610	25563236.943	0.011	0.010	60.030
0.610	25606610.460	0.011	0.010	59.783
0.630	89.306	0.146	0.236	20.352
0.566	857.880	0.325	0.123	59.817
0.554	75.110	0.137	0.234	18.373
0.558	1671.698	0.329	0.028	60.148
0.540	3106.172	0.011	0.010	60.150
0.586	145.809	0.277	0.241	48.830
0.534	119.035	0.245	0.243	41.579
0.553	2302.187	0.012	0.011	59.864
0.549	5489.405	0.011	0.010	60.039
0.556	4930.388	0.011	0.010	60.138
0.550	117.941	0.238	0.245	39.024
0.558	123.184	0.244	0.245	41.421
0.578	47609.086	0.011	0.010	59.952
0.592	413975.093	0.011	0.010	60.085
0.570	78649.224	0.012	0.011	60.044
0.586	91365.228	0.011	0.010	60.084
0.584	103279.399	0.011	0.010	60.254
0.594	274730.446	0.012	0.011	59.845
0.569	574025.837	0.011	0.010	59.853
0.560	2584066.466	0.011	0.010	60.141
0.562	1003771.740	0.011	0.010	60.276
0.572	220.320	0.325	0.221	60.053
0.558	174.850	0.321	0.235	58.520
0.587	243.090	0.324	0.217	59.788
0.586	3990.793	0.012	0.012	59.777
0.586	254.628	0.426	0.214	59.904
0.597	427.163	0.411	0.189	59.977
0.583	138.993	0.264	0.244	45.625

0.589	1075.528	0.327	0.107	59.876
0.597	333.033	0.327	0.197	59.862
0.594	174.016	0.390	0.238	54.977
0.606	255.586	0.327	0.217	60.453
0.588	409.502	0.325	0.193	60.066
0.583	1803.392	0.341	0.025	59.947
0.581	2766.437	0.011	0.010	59.889
0.587	526.902	0.324	0.167	59.892
0.585	1377.746	0.390	0.059	60.978
0.580	478.926	0.328	0.177	60.064
0.574	743.051	0.326	0.135	59.969
0.579	11139.248	0.011	0.012	59.871
0.574	786.256	0.410	0.167	59.945
0.578	583.283	0.329	0.156	59.895
0.579	11424.387	0.011	0.011	60.080
0.574	2772.724	0.013	0.010	59.908
0.569	2880.978	0.011	0.010	59.845
0.566	10376.718	0.011	0.010	59.755
0.564	799.297	0.325	0.129	59.749
0.569	1235.860	0.327	0.075	60.027
0.566	626.846	0.326	0.149	60.472
0.570	542.040	0.326	0.160	59.901
0.571	1234.085	0.323	0.076	59.821
0.568	4631.618	0.011	0.010	59.831
0.565	1466.515	0.326	0.042	60.047
0.568	1987.540	0.275	0.017	60.020
0.569	48213.850	0.011	0.010	60.314
0.570	136995.729	0.011	0.010	59.886
0.570	144080.931	0.011	0.010	59.836
0.569	1948.204	0.264	0.018	60.542
0.571	1312.999	0.325	0.065	59.948
0.572	806.040	0.328	0.128	60.399
0.574	572.362	0.326	0.155	59.958
0.572	557.630	0.327	0.157	59.927
0.572	432.613	0.334	0.185	60.046
0.573	542.463	0.326	0.159	59.713
0.575	545.703	0.325	0.160	59.838
0.573	573.761	0.325	0.154	60.125

0.572	501.349	0.327	0.169	60.113
0.574	465.697	0.328	0.177	59.896
0.573	468.337	0.326	0.176	59.850
0.575	435.355	0.326	0.184	59.939
0.575	374.840	0.333	0.203	60.052
0.575	420.821	0.326	0.186	59.707
0.575	425.710	0.328	0.185	59.889
0.574	401.708	0.326	0.193	60.065
0.574	358.447	0.326	0.193	59.869
0.575	333.108	0.326	0.195	59.896
0.575	333.166	0.328	0.198	60.589
0.575	353.675	0.331	0.197	59.874
0.638	3.582	0.074	0.081	1.820
0.108	0.025	0.073	0.062	1.334
0.680	2.047	0.073	0.071	1.642
0.701	1.658	0.073	0.070	1.602
0.852	0.455	0.074	0.065	1.393
0.853	0.450	0.072	0.064	1.397
0.948	4505.320	0.011	0.012	59.874
0.947	0.134	0.072	0.061	1.320
0.109	333.574	0.324	0.036	59.804
0.217	1.565	0.074	0.087	1.897
0.015	333.668	0.011	0.010	59.820
0.013	0.092	0.074	0.086	1.882
0.012	333.671	0.011	0.010	59.878
0.013	367.666	0.011	0.010	59.848
0.942	0.059	0.073	0.061	1.290
0.377	16251.645	0.011	0.010	60.019
0.044	16251.978	0.011	0.010	59.759
0.313	16251.709	0.011	0.010	59.937
0.590	0.872	0.073	0.069	1.523
0.307	16.801	0.081	0.179	4.562
0.319	16695.636	0.011	0.010	60.323
0.375	4.145	0.074	0.097	2.071
0.540	1.123	0.075	0.070	1.606
0.111	16695.844	0.011	0.010	59.920
0.153	24093.251	0.011	0.012	59.800
0.628	0.491	0.072	0.063	1.437

0.211	35564.748	0.011	0.010	60.149
0.535	153162.652	0.011	0.012	59.785
0.142	153163.045	0.013	0.012	59.861
0.528	42.360	0.090	0.205	6.812
0.233	0.181	0.072	0.064	1.440
0.937	1972063.144	0.011	0.010	59.885
0.939	2064539.972	0.011	0.010	59.991
0.213	0.063	0.072	0.061	1.365
0.961	3269697.873	0.011	0.010	59.751
0.935	0.528	0.073	0.065	1.409
0.999	100305862.002	0.011	0.010	60.421
1.000	0.369	0.107	0.094	1.942
0.999	8.815	0.077	0.102	2.023
0.395	0.258	0.073	0.064	1.435
0.264	100305864.088	0.011	0.010	60.024
0.643	0.607	0.072	0.064	1.473
0.174	100305866.518	0.011	0.010	59.964
0.051	100305859.672	0.011	0.010	59.945
0.583	389802175.206	0.011	0.010	59.784
0.816	1238304619.480	0.011	0.010	59.949
0.998	7.432	0.074	0.088	1.897
0.624	1238304742.614	0.011	0.010	59.872
0.289	1238304607.734	0.011	0.011	64.326
0.374	0.559	0.074	0.067	1.539
0.290	1238305067.888	0.011	0.010	59.986
0.943	12431436516.883	0.011	0.010	60.097
0.950	14039333726.857	0.011	0.010	60.009
0.125	0.019	0.074	0.062	1.320
0.697	21.957	0.077	0.149	3.264
0.214	12431403439.504	0.012	0.011	60.111
0.172	1.088	0.078	0.082	1.860
0.083	0.053	0.072	0.067	1.439
0.141	1.554	0.076	0.098	2.081
0.679	0.469	0.074	0.064	1.447
0.064	12431404282.618	0.011	0.010	60.442
0.073	14351558608.642	0.012	0.010	60.174
0.067	14351565920.868	0.012	0.010	60.020
0.046	14351342343.463	0.011	0.010	60.107

0.002	14356458634.012	0.011	0.010	60.213
0.059	0.472	0.075	0.088	1.933
0.707	437608603363.030	0.011	0.010	60.143
0.556	2.206	0.074	0.075	1.716
0.247	437638177912.578	0.011	0.010	59.940
0.071	0.048	0.071	0.063	1.439
0.425	983000350018.705	0.011	0.010	59.962
0.015	0.001	0.072	0.061	1.282
0.554	1654752627607.720	0.011	0.010	59.826
0.399	1654443854224.937	0.013	0.011	59.882
0.578	1.620	0.073	0.071	1.628
0.218	0.453	0.072	0.069	1.599
0.185	1654340747946.818	0.011	0.010	60.414
0.172	0.010	0.074	0.061	1.277
0.450	14995320114410.135	0.011	0.010	60.130
0.363	25517193203125.410	0.011	0.010	59.815
0.173	0.880	0.074	0.078	1.786
0.790	69054394882060.875	0.011	0.010	60.223
0.945	315181511210923.438	0.011	0.010	60.278
0.993	1.185	0.072	0.066	1.508
0.700	71648395791194.875	0.011	0.010	60.262
0.606	72765966940099.734	0.013	0.012	65.134
0.583	72935167690834.531	0.011	0.010	62.629
0.124	0.238	0.075	0.071	1.619
0.100	0.306	0.077	0.075	1.697
0.905	1.309	0.074	0.068	1.545
0.324	108131269360043.281	0.012	0.012	61.409
0.692	346167760772437.875	0.012	0.010	60.630
0.286	0.575	0.074	0.071	1.599
0.931	3.003	0.074	0.072	1.719
0.820	1.694	0.075	0.071	1.630
0.313	0.849	0.082	0.078	1.700
0.660	198135846416405.500	0.012	0.011	61.229
0.427	Inf	0.007	0.007	0.073
0.289	1.808	0.073	0.082	1.851
0.797	1795102608937774.500	0.012	0.011	61.665
0.425	127618920865804.078	0.011	0.010	59.719
0.558	86606009446530.328	0.013	0.012	65.292

0.324	2.279	0.073	0.085	1.887
0.704	2.681	0.077	0.076	1.728
0.410	205039104325113.406	0.011	0.010	60.376
0.596	3.954	0.075	0.086	1.883
0.434	976772559098846.875	0.013	0.011	60.741
0.462	1387571391743837.250	0.011	0.010	60.637
0.344	1.844	0.075	0.081	1.807
0.280	10.000	0.075	0.154	3.451
0.385	1731637467187315.500	0.013	0.010	60.275
0.236	Inf	0.008	0.007	0.075
0.387	1744183808921576.750	0.011	0.010	60.712
0.533	14.568	0.076	0.143	3.150
0.392	2.294	0.075	0.083	1.873
0.387	3490055779486240.000	0.011	0.010	61.044
0.411	Inf	0.008	0.007	0.078
0.444	Inf	0.007	0.007	0.075
0.359	4.098	0.078	0.102	2.136
0.481	Inf	0.008	0.007	0.077
0.407	Inf	0.008	0.007	0.077
0.538	Inf	0.007	0.007	0.074
0.599	Inf	0.008	0.007	0.075
0.684	23.373	0.079	0.157	3.494
0.526	11.017	0.076	0.125	2.705
0.583	6.574	0.078	0.099	2.105
0.641	Inf	0.007	0.007	0.075
0.574	Inf	0.008	0.007	0.073
0.612	Inf	0.007	0.007	0.073
0.533	Inf	0.008	0.007	0.074
0.562	9.390	0.076	0.113	2.430
0.533	Inf	0.008	0.007	0.076
0.518	Inf	0.007	0.007	0.074
0.514	Inf	0.008	0.007	0.076
0.556	15.373	0.076	0.151	3.147
0.524	Inf	0.008	0.007	0.076
0.515	Inf	0.007	0.007	0.075
0.503	Inf	0.008	0.007	0.077
0.507	Inf	0.008	0.007	0.082
0.506	Inf	0.008	0.007	0.077

0.506	Inf	0.007	0.007	0.074
0.480	18.658	0.082	0.167	4.288
0.502	14.056	0.081	0.151	4.091
0.524	Inf	0.008	0.008	0.090
0.536	Inf	0.010	0.009	0.089
0.541	Inf	0.008	0.007	0.082
0.549	Inf	0.007	0.007	0.076
0.524	Inf	0.008	0.008	0.086
0.555	21.891	0.083	0.166	3.734
0.566	32.116	0.085	0.185	4.834
0.554	Inf	0.007	0.007	0.077
0.548	25.582	0.085	0.183	4.334
0.554	Inf	0.010	0.009	0.087
0.564	32.554	0.103	0.233	5.792
0.546	Inf	0.009	0.010	0.092
0.571	122.756	0.296	0.286	43.774
0.547	Inf	0.008	0.007	0.081
0.556	Inf	0.007	0.007	0.074
0.547	Inf	0.008	0.007	0.076
0.533	262.769	0.343	0.214	61.596
0.547	Inf	0.007	0.007	0.076
0.535	149.540	0.308	0.261	53.073
0.552	Inf	0.008	0.007	0.081
0.554	Inf	0.008	0.007	0.165
0.554	Inf	0.022	0.013	0.126
0.551	52.229	0.127	0.401	9.820
0.561	79.935	0.147	0.236	20.484
0.563	589.484	0.366	0.167	60.885
0.569	77.429	0.140	0.235	18.601
0.563	703.822	0.327	0.140	60.057
0.570	7249.694	0.014	0.014	67.599
0.563	148.459	0.292	0.263	51.802
0.566	93.029	0.175	0.255	25.526
0.576	236.341	0.327	0.220	60.399
0.570	284.889	0.329	0.210	59.895
0.572	72.840	0.128	0.236	16.388
0.571	342.116	0.362	0.200	60.737
0.565	309.761	0.338	0.209	61.793

0.575	114.384	0.222	0.261	34.206
0.566	4001.572	0.011	0.011	60.681
0.568	100.484	0.191	0.254	28.568
0.575	327.304	0.330	0.200	60.327
0.575	380.625	0.428	0.256	62.713
0.577	118.916	0.223	0.250	36.697
0.571	327.352	0.328	0.197	59.732
0.570	603.347	0.335	0.156	60.939
0.573	484.232	0.337	0.179	61.689
0.572	1122.072	0.355	0.104	62.260
0.572	151.569	0.346	0.248	52.487
0.571	2096.707	0.140	0.014	59.916
0.568	75231.410	0.012	0.011	60.640
0.570	4429.231	0.011	0.011	60.451
0.572	223.579	0.333	0.228	61.243
0.574	185.610	0.332	0.242	60.686
0.574	135.712	0.269	0.249	45.943
0.570	285.671	0.329	0.210	61.182
0.568	313.581	0.335	0.204	60.977
0.569	20881.920	0.011	0.010	60.691
0.571	160.546	0.306	0.240	53.442
0.568	410.242	0.337	0.194	60.758
0.567	1370.007	0.332	0.058	60.947
0.568	186.484	0.332	0.234	60.013
0.567	2923.494	0.011	0.010	60.616
0.567	331.922	0.333	0.198	60.422
0.567	2058.028	0.201	0.016	61.083
0.566	2485.140	0.012	0.011	60.504
0.566	373.726	0.327	0.194	60.560
0.565	1929.240	0.264	0.019	60.435
0.565	1191.799	0.328	0.084	59.982
0.565	371.721	0.329	0.194	60.762
0.565	1200.411	0.341	0.087	60.770
0.565	434.160	0.331	0.185	61.600
0.565	994.705	0.335	0.112	61.263
0.566	5608.364	0.011	0.010	60.755
0.565	30243.499	0.011	0.010	60.744
0.565	18656.519	0.011	0.011	60.400

0.566	829.964	0.331	0.127	60.595
0.565	1808.195	0.332	0.025	60.610
0.566	1118.548	0.339	0.096	60.318
0.565	810.519	0.332	0.128	60.242
0.566	539.746	0.329	0.163	60.540
0.565	486.701	0.328	0.173	61.309
0.565	463.066	0.329	0.177	61.302
0.565	463.148	0.334	0.183	61.101
0.565	504.532	0.332	0.173	61.540
0.181	0.085	0.074	0.065	1.414
0.054	0.006	0.075	0.062	1.316
0.592	517.563	0.329	0.170	61.272
0.586	Inf	0.007	0.007	0.074
0.615	Inf	0.007	0.006	0.073
0.615	11.683	0.076	0.121	2.602
0.608	23.695	0.078	0.163	3.657
0.604	47.709	0.091	0.209	6.846
0.602	95.731	0.164	0.252	24.160
0.601	191.771	0.326	0.240	59.818
0.601	383.851	0.332	0.200	61.761
0.571	365.141	0.333	0.197	61.223
0.556	Inf	0.007	0.007	0.078
0.590	502.546	0.332	0.173	61.179
0.580	538.899	0.336	0.172	61.426
0.596	6099.397	0.011	0.010	60.958
0.584	702.440	0.329	0.143	60.591
0.587	739.338	0.327	0.140	60.487
0.582	15893.910	0.011	0.010	61.014
0.586	968.954	0.333	0.118	60.726
0.585	1032.172	0.335	0.111	60.304
0.587	15382.193	0.011	0.010	61.248
0.585	1347.418	0.330	0.065	60.386
0.586	1425.487	0.329	0.058	61.889
0.585	24942.484	0.011	0.010	60.046
0.585	4866.317	0.013	0.012	62.095
0.585	2367.957	0.011	0.010	60.577
0.585	3809.873	0.011	0.010	60.159
0.585	9735.906	0.011	0.010	60.803

0.585	4737.682	0.011	0.010	60.795
0.585	7621.808	0.011	0.010	61.450
0.586	19475.083	0.011	0.010	60.132
0.586	9477.134	0.011	0.010	59.727
0.586	Inf	0.007	0.006	0.073
0.586	145.000	0.277	0.244	49.277
0.000	Inf	0.007	0.006	0.073
